are widely used in the study of electromechanical-energy-conversion devices and form the basis for most of the analyses presented here.

1.1 INTRODUCTION TO MAGNETIC CIRCUITS

The complete, detailed solution for magnetic fields in most situations of practical engineering interest involves the solution of Maxwell's equations and requires a set of constitutive relationships to describe material properties. Although in practice exact solutions are often unattainable, various simplifying assumptions permit the attainment of useful engineering solutions.[1]

We begin with the assumption that, for the systems treated in this book, the frequencies and sizes involved are such that the displacement-current term in Maxwell's equations can be neglected. This term accounts for magnetic fields being produced in space by time-varying electric fields and is associated with electromagnetic radiation. Neglecting this term results in the magneto-quasi-static form of the relevant Maxwell's equations which relate magnetic fields to the currents which produce them.

$$\oint_C \mathbf{H}\mathbf{dl} = \int_S \mathbf{J} \cdot \mathbf{da} \tag{1.1}$$

$$\oint_S \mathbf{B} \cdot \mathbf{da} = 0 \tag{1.2}$$

Equation 1.1, frequently referred to as *Ampere's Law*, states that the line integral of the tangential component of the *magnetic field intensity* $\mathbf{H}$ around a closed contour C is equal to the total current passing through any surface S linking that contour. From Eq. 1.1 we see that the source of $\mathbf{H}$ is the *current density* $\mathbf{J}$. Eq. 1.2, frequently referred to as *Gauss' Law for magnetic fields*, states that *magnetic flux density* $\mathbf{B}$ is conserved, i.e., that no net flux enters or leaves a closed surface (this is equivalent to saying that there exist no monopolar sources of magnetic fields). From these equations we see that the magnetic field quantities can be determined solely from the instantaneous values of the source currents and hence that time variations of the magnetic fields follow directly from time variations of the sources.

A second simplifying assumption involves the concept of a *magnetic circuit*. It is extremely difficult to obtain the general solution for the magnetic field intensity $\mathbf{H}$ and the magnetic flux density $\mathbf{B}$ in a structure of complex geometry. However, in many practical applications, including the analysis of many types of electric machines, a three-dimensional field problem can often be approximated by what is essentially

[1] Computer-based numerical solutions based upon the finite-element method form the basis for a number of commercial programs and have become indispensable tools for analysis and design. Such tools are typically best used to refine initial analyses based upon analytical techniques such as are found in this book. Because such techniques contribute little to a fundamental understanding of the principles and basic performance of electric machines, they are not discussed in this book.

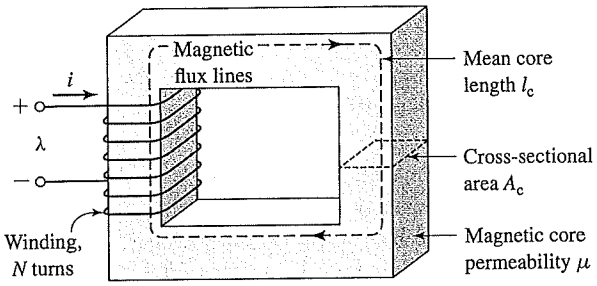

Figure 1.1 Simple magnetic circuit. λ is the winding flux linkage as defined in Section 1.2.

a one-dimensional circuit equivalent, yielding solutions of acceptable engineering accuracy.

A magnetic circuit consists of a structure composed for the most part of high-permeability magnetic material.[2] The presence of high-permeability material tends to cause magnetic flux to be confined to the paths defined by the structure, much as currents are confined to the conductors of an electric circuit. Use of this concept of the magnetic circuit is illustrated in this section and will be seen to apply quite well to many situations in this book.[3]

A simple example of a magnetic circuit is shown in Fig. 1.1. The core is assumed to be composed of magnetic material whose *magnetic permeability* μ is much greater than that of the surrounding air ($\mu \gg \mu_0$) where $\mu_0 = 4\pi \times 10^{-7}$ H/m is the magnetic permeability of free space. The core is of uniform cross section and is excited by a winding of N turns carrying a current of i amperes. This winding produces a magnetic field in the core, as shown in the figure.

Because of the high permeability of the magnetic core, an exact solution would show that the magnetic flux is confined almost entirely to the core, with the field lines following the path defined by the core, and that the flux density is essentially uniform over a cross section because the cross-sectional area is uniform. The magnetic field can be visualized in terms of flux lines which form closed loops interlinked with the winding.

As applied to the magnetic circuit of Fig. 1.1, the source of the magnetic field in the core is the ampere-turn product Ni. In magnetic circuit terminology Ni is the *magnetomotive force* (mmf) $\mathcal{F}$ acting on the magnetic circuit. Although Fig. 1.1 shows only a single winding, transformers and most rotating machines typically have at least two windings, and Ni must be replaced by the algebraic sum of the ampere-turns of all the windings.

---

[2] In its simplest definition, magnetic permeability can be thought of as the ratio of the magnitude of the magnetic flux density B to the magnetic field intensity H.

[3] For a more extensive treatment of magnetic circuits see A.E. Fitzgerald, D.E. Higgenbotham, and A. Grabel, *Basic Electrical Engineering*, 5th ed., McGraw-Hill, 1981, chap. 13; also E.E. Staff, M.I.T., *Magnetic Circuits and Transformers*, M.I.T. Press, 1965, chaps. 1 to 3.

The net *magnetic flux* ϕ crossing a surface S is the surface integral of the normal component of **B**; thus

$$\phi = \int_S \mathbf{B} \cdot \mathbf{da} \tag{1.3}$$

In SI units, the unit of ϕ is the *weber* (Wb).

Equation 1.2 states that the net magnetic flux entering or leaving a closed surface (equal to the surface integral of **B** over that closed surface) is zero. This is equivalent to saying that all the flux which enters the surface enclosing a volume must leave that volume over some other portion of that surface because magnetic flux lines form closed loops. Because little flux "leaks" out the sides of the magnetic circuit of Fig. 1.1, this result shows that the net flux is the same through each cross section of the core.

For a magnetic circuit of this type, it is common to assume that the magnetic flux density (and correspondingly the magnetic field intensity) is uniform across the cross section and throughout the core. In this case Eq. 1.3 reduces to the simple scalar equation

$$\phi_c = B_c A_c \tag{1.4}$$

where

ϕ_c = core flux
B_c = core flux density
A_c = core cross-sectional area

From Eq. 1.1, the relationship between the mmf acting on a magnetic circuit and the magnetic field intensity in that circuit is.[4]

$$\mathcal{F} = Ni = \oint \mathbf{Hdl} \tag{1.5}$$

The core dimensions are such that the path length of any flux line is close to the mean core length l_c. As a result, the line integral of Eq. 1.5 becomes simply the scalar product $H_c l_c$ of the magnitude of **H** and the mean flux path length l_c. Thus, the relationship between the mmf and the magnetic field intensity can be written in magnetic circuit terminology as

$$\mathcal{F} = Ni = H_c l_c \tag{1.6}$$

where H_c is average magnitude of **H** in the core.

The direction of H_c in the core can be found from the *right-hand rule*, which can be stated in two equivalent ways. (1) Imagine a current-carrying conductor held in the right hand with the thumb pointing in the direction of current flow; the fingers then point in the direction of the magnetic field created by that current. (2) Equivalently, if the coil in Fig. 1.1 is grasped in the right hand (figuratively speaking) with the fingers

[4] In general, the mmf drop across any segment of a magnetic circuit can be calculated as $\int$ **Hdl** over that portion of the magnetic circuit.

pointing in the direction of the current, the thumb will point in the direction of the magnetic fields.

The relationship between the magnetic field intensity **H** and the magnetic flux density **B** is a property of the material in which the field exists. It is common to assume a linear relationship; thus

$$\mathbf{B} = \mu\mathbf{H} \tag{1.7}$$

where μ is the material's magnetic permeability. In SI units, **H** is measured in units of *amperes per meter*, **B** is in *webers per square meter*, also known as *teslas* (T), and μ is in *webers per ampere-turn-meter*, or equivalently *henrys per meter*. In SI units the permeability of free space is $\mu_0 = 4\pi \times 10^{-7}$ henrys per meter. The permeability of linear magnetic material can be expressed in terms of its *relative permeability* μ_r, its value relative to that of free space; $\mu = \mu_r\mu_0$. Typical values of μ_r range from 2,000 to 80,000 for materials used in transformers and rotating machines. The characteristics of ferromagnetic materials are described in Sections 1.3 and 1.4. For the present we assume that μ_r is a known constant, although it actually varies appreciably with the magnitude of the magnetic flux density.

Transformers are wound on closed cores like that of Fig. 1.1. However, energy conversion devices which incorporate a moving element must have air gaps in their magnetic circuits. A magnetic circuit with an air gap is shown in Fig. 1.2. When the air-gap length g is much smaller than the dimensions of the adjacent core faces, the core flux ϕ_c will follow the path defined by the core and the air gap and the techniques of magnetic-circuit analysis can be used. If the air-gap length becomes excessively large, the flux will be observed to "leak out" of the sides of the air gap and the techniques of magnetic-circuit analysis will no longer be strictly applicable.

Thus, provided the air-gap length g is sufficiently small, the configuration of Fig. 1.2 can be analyzed as a magnetic circuit with two series components both carrying the same flux ϕ: a magnetic core of permeability μ, cross-sectional area A_c and mean length l_c, and an air gap of permeability μ_0, cross-sectional area A_g and length g. In the core

$$B_c = \frac{\phi}{A_c} \tag{1.8}$$

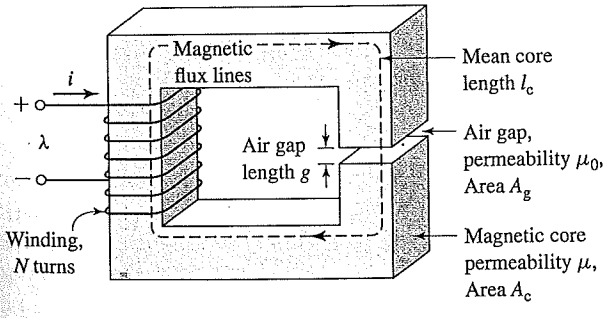

Figure 1.2 Magnetic circuit with air gap.

and in the air gap

$$B_g = \frac{\phi}{A_c} \tag{1.9}$$

Application of Eq. 1.5 to this magnetic circuit yields

$$\mathcal{F} = H_c l_c + H_g g \tag{1.10}$$

and using the linear B-H relationship of Eq. 1.7 gives

$$\mathcal{F} = \frac{B_c}{\mu} l_c + \frac{B_g}{\mu_0} g \tag{1.11}$$

Here the $\mathcal{F} = Ni$ is the mmf applied to the magnetic circuit. From Eq. 1.10 we see that a portion of the mmf, $\mathcal{F}_c = H_c l_c$, is required to produce magnetic field in the core while the remainder, $\mathcal{F}_g = H_g g$ produces magnetic field in the air gap.

For practical magnetic materials (as is discussed in Sections 1.3 and 1.4), B_c and H_c are not simply related by a known constant permeability μ as described by Eq. 1.7. In fact, B_c is often a nonlinear, multi-valued function of H_c. Thus, although Eq. 1.10 continues to hold, it does not lead directly to a simple expression relating the mmf and the flux densities, such as that of Eq. 1.11. Instead the specifics of the nonlinear B_c-H_c relation must be used, either graphically or analytically. However, in many cases, the concept of constant material permeability gives results of acceptable engineering accuracy and is frequently used.

From Eqs. 1.8 and 1.9, Eq. 1.11 can be rewritten in terms of the flux ϕ_c as

$$\mathcal{F} = \phi \left(\frac{l_c}{\mu A_c} + \frac{g}{\mu_0 A_g} \right) \tag{1.12}$$

The terms that multiply the flux in this equation are known as the *reluctance* ($\mathcal{R}$) of the core and air gap, respectively,

$$\mathcal{R}_c = \frac{l_c}{\mu A_c} \tag{1.13}$$

$$\mathcal{R}_g = \frac{g}{\mu_0 A_g} \tag{1.14}$$

and thus

$$\mathcal{F} = \phi(\mathcal{R}_c + \mathcal{R}_g) \tag{1.15}$$

Finally, Eq. 1.15 can be inverted to solve for the flux

$$\phi = \frac{\mathcal{F}}{\mathcal{R}_c + \mathcal{R}_g} \tag{1.16}$$

or

$$\phi = \frac{\mathcal{F}}{\frac{l_c}{\mu A_c} + \frac{g}{\mu_0 A_g}} \tag{1.17}$$

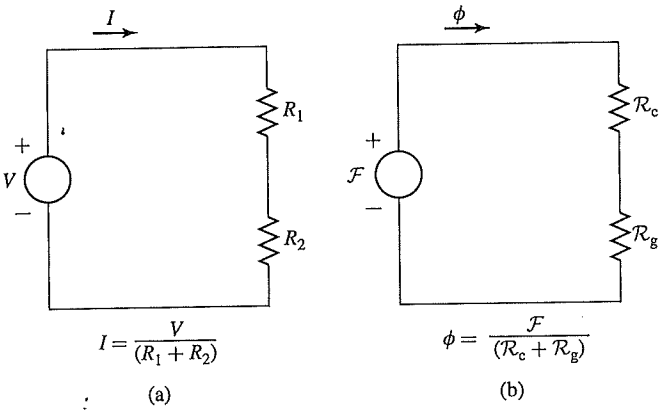

Figure 1.3 Analogy between electric and magnetic circuits. (a) Electric circuit. (b) Magnetic circuit.

In general, for any magnetic circuit of total reluctance $\mathcal{R}_{tot}$, the flux can be found as

$$\phi = \frac{\mathcal{F}}{\mathcal{R}_{tot}} \tag{1.18}$$

The term which multiplies the mmf is known as the *permeance* $\mathcal{P}$ and is the inverse of the reluctance; thus, for example, the total permeance of a magnetic circuit is

$$\mathcal{P}_{tot} = \frac{1}{\mathcal{R}_{tot}} \tag{1.19}$$

Note that Eqs. 1.15 and 1.16 are analogous to the relationships between the current and voltage in an electric circuit. This analogy is illustrated in Fig. 1.3. Figure 1.3a shows an electric circuit in which a voltage V drives a current I through resistors R_1 and R_2. Figure 1.3b shows the schematic equivalent representation of the magnetic circuit of Fig. 1.2 . Here we see that the mmf $\mathcal{F}$ (analogous to voltage in the electric circuit) drives a flux ϕ (analogous to the current in the electric circuit) through the combination of the reluctances of the core $\mathcal{R}_c$ and the air gap $\mathcal{R}_g$. This analogy between the solution of electric and magnetic circuits can often be exploited to produce simple solutions for the fluxes in magnetic circuits of considerable complexity.

The fraction of the mmf required to drive flux through each portion of the magnetic circuit, commonly referred to as the *mmf drop* across that portion of the magnetic circuit, varies in proportion to its reluctance (directly analogous to the voltage drop across a resistive element in an electric circuit). Consider the magnetic circuit of Fig. 1.2. From Eq. 1.13 we see that high material permeability can result in low core reluctance, which can often be made much smaller than that of the air gap; i.e., for $(\mu A_c/l_c) \gg (\mu_0 A_g/g)$, $\mathcal{R}_c \ll \mathcal{R}_g$ and thus $\mathcal{R}_{tot} \approx \mathcal{R}_g$. In this case, the reluctance of the core can be neglected and the flux can be found from Eq. 1.16 in terms of $\mathcal{F}$ and the air-gap properties alone:

$$\phi \approx \frac{\mathcal{F}}{\mathcal{R}_g} = \frac{\mathcal{F}\mu_0 A_g}{g} = Ni\,\frac{\mu_0 A_g}{g} \tag{1.20}$$

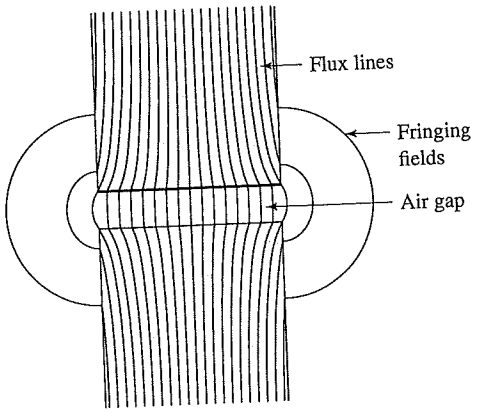

Figure 1.4 Air-gap fringing fields.

As will be seen in Section 1.3, practical magnetic materials have permeabilities which are not constant but vary with the flux level. From Eqs. 1.13 to 1.16 we see that as long as this permeability remains sufficiently large, its variation will not significantly affect the performance of a magnetic circuit in which the dominant reluctance is that of an air gap.

In practical systems, the magnetic field lines "fringe" outward somewhat as they cross the air gap, as illustrated in Fig. 1.4. Provided this fringing effect is not excessive, the magnetic-circuit concept remains applicable. The effect of these *fringing fields* is to increase the effective cross-sectional area A_g of the air gap. Various empirical methods have been developed to account for this effect. A correction for such fringing fields in short air gaps can be made by adding the gap length to each of the two dimensions making up its cross-sectional area. In this book the effect of fringing fields is usually ignored. If fringing is neglected, $A_g = A_c$.

In general, magnetic circuits can consist of multiple elements in series and parallel. To complete the analogy between electric and magnetic circuits, we can generalize Eq. 1.5 as

$$\mathcal{F} = \oint \mathbf{H}\mathbf{dl} = \sum_k \mathcal{F}_k = \sum_k H_k l_k \tag{1.21}$$

where $\mathcal{F}$ is the mmf (total ampere-turns) acting to drive flux through a closed loop of a magnetic circuit, and $\mathcal{F}_k = H_k l_k$ is the *mmf drop* across the k'th element of that loop. This is directly analogous to Kirchoff's voltage law for electric circuits consisting of voltage sources and resistors

$$V = \sum_k R_k i_k \tag{1.22}$$

where V is the source voltage driving current around a loop and $R_k i_k$ is the voltage drop across the k'th resistive element of that loop.

Similarly, the analogy to Kirchoff's current law

$$\sum_n i_n = 0 \tag{1.23}$$

which says that the net current, i.e. the sum of the currents, into a node in an electric circuit equals zero is

$$\sum_n \phi_n = 0 \tag{1.24}$$

which states that the net flux into a node in a magnetic circuit is zero.

We have now described the basic principles for reducing a magneto-quasi-static field problem with simple geometry to a *magnetic circuit model*. Our limited purpose in this section is to introduce some of the concepts and terminology used by engineers in solving practical design problems. We must emphasize that this type of thinking depends quite heavily on engineering judgment and intuition. For example, we have tacitly assumed that the permeability of the "iron" parts of the magnetic circuit is a constant known quantity, although this is not true in general (see Section 1.3), and that the magnetic field is confined solely to the core and its air gaps. Although this is a good assumption in many situations, it is also true that the winding currents produce magnetic fields outside the core. As we shall see, when two or more windings are placed on a magnetic circuit, as happens in the case of both transformers and rotating machines, these fields outside the core, referred to as *leakage fields*, cannot be ignored and may significantly affect the performance of the device.

EXAMPLE 1.1

The magnetic circuit shown in Fig. 1.2 has dimensions $A_c = A_g = 9$ cm^2, $g = 0.050$ cm, $l_c = 30$ cm, and $N = 500$ turns. Assume the value $\mu_r = 70{,}000$ for core material. (a) Find the reluctances $\mathcal{R}_c$ and $\mathcal{R}_g$. For the condition that the magnetic circuit is operating with $B_c = 1.0$ T, find (b) the flux ϕ and (c) the current i.

■ Solution

a. The reluctances can be found from Eqs. 1.13 and 1.14:

$$\mathcal{R}_c = \frac{l_c}{\mu_r \mu_0 A_c} = \frac{0.3}{70,000\,(4\pi \times 10^{-7})(9 \times 10^{-4})} = 3.79 \times 10^3 \quad \frac{\text{A} \cdot \text{turns}}{\text{Wb}}$$

$$\mathcal{R}_g = \frac{g}{\mu_0 A_g} = \frac{5 \times 10^{-4}}{(4\pi \times 10^{-7})(9 \times 10^{-4})} = 4.42 \times 10^5 \quad \frac{\text{A} \cdot \text{turns}}{\text{Wb}}$$

b. From Eq. 1.4,

$$\phi = B_c A_c = 1.0(9 \times 10^{-4}) = 9 \times 10^{-4} \text{ Wb}$$

c. From Eqs. 1.6 and 1.15,

$$i = \frac{\mathcal{F}}{N} = \frac{\phi(\mathcal{R}_c + \mathcal{R}_g)}{N} = \frac{9 \times 10^{-4}(4.46 \times 10^5)}{500} = 0.80 \text{ A}$$

Practice Problem 1.1

Find the flux ϕ and current for Example 1.1 if (a) the number of turns is doubled to $N = 1000$ turns while the circuit dimensions remain the same and (b) if the number of turns is equal to $N = 500$ and the gap is reduced to 0.040 cm.

Solution

a. $\phi = 9 \times 10^{-4}$ Wb and $i = 0.40$ A
b. $\phi = 9 \times 10^{-4}$ Wb and $i = 0.64$ A

EXAMPLE 1.2

The magnetic structure of a synchronous machine is shown schematically in Fig. 1.5. Assuming that rotor and stator iron have infinite permeability ($\mu \to \infty$), find the air-gap flux ϕ and flux density B_g. For this example $I = 10$ A, $N = 1{,}000$ turns, $g = 1$ cm, and $A_g = 200$ cm^2.

Solution

Notice that there are two air gaps in series, of total length $2g$, and that by symmetry the flux density in each is equal. Since the iron permeability is assumed to be infinite, its reluctance is negligible and Eq. 1.20 (with g replaced by the total gap length $2g$) can be used to find the flux

$$\phi = \frac{NI\mu_0 A_g}{2g} = \frac{1000(10)(4\pi \times 10^{-7})(0.02)}{0.02} = 12.6 \text{ m Wb}$$

and

$$B_g = \frac{\phi}{A_g} = \frac{0.0126}{0.02} = 0.630 \text{ T}$$

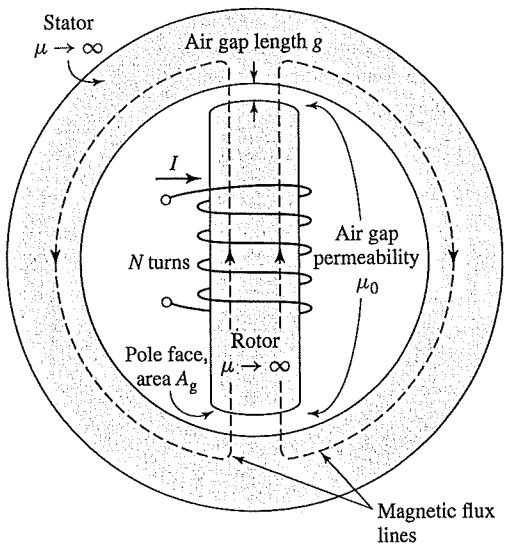

Figure 1.5 Simple synchronous machine.

Practice Problem 1.2

For the magnetic structure of Fig. 1.5 with the dimensions as given in Example 1.2, the air-gap flux density is observed to be $B_g = 0.9$ T. Find the air-gap flux ϕ and, for a coil of $N = 500$ turns, the current required to produce this level of air-gap flux.

Solution

$\phi = 0.018$ Wb and $i = 28.6$ A.

1.2 FLUX LINKAGE, INDUCTANCE, AND ENERGY

When a magnetic field varies with time, an electric field is produced in space as determined by another of Maxwell's equations referred to as *Faraday's law*:

$$\oint_C \mathbf{E} \cdot \mathbf{ds} = -\frac{d}{dt} \int_S \mathbf{B} \cdot \mathbf{da} \tag{1.25}$$

Equation 1.25 states that the line integral of the *electric field intensity* $\mathbf{E}$ around a closed contour C is equal to the time rate of change of the magnetic flux linking (i.e., passing through) that contour. In magnetic structures with windings of high electrical conductivity, such as in Fig. 1.2, it can be shown that the $\mathbf{E}$ field in the wire is extremely small and can be neglected, so that the left-hand side of Eq. 1.25 reduces to the negative of the *induced voltage*[5] e at the winding terminals. In addition, the flux on the right-hand side of Eq. 1.25 is dominated by the core flux ϕ. Since the winding (and hence the contour C) links the core flux N times, Eq. 1.25 reduces to

$$e = N\frac{d\varphi}{dt} = \frac{d\lambda}{dt} \tag{1.26}$$

where λ is the *flux linkage* of the winding and is defined as

$$\lambda = N\varphi \tag{1.27}$$

Flux linkage is measured in units of webers (or equivalently weber-turns). Note that we have chosen the symbol φ to indicate the instantaneous value of a time-varying flux.

In general the flux linkage of a coil is equal to the surface integral of the normal component of the magnetic flux density integrated over any surface spanned by that coil. Note that the direction of the induced voltage e is defined by Eq. 1.25 so that if the winding terminals were short-circuited, a current would flow in such a direction as to oppose the change of flux linkage.

For a magnetic circuit composed of magnetic material of constant magnetic permeability or which includes a dominating air gap, the relationship between λ

[5] The term *electromotive force* (emf) is often used instead of induced voltage to represent that component of voltage due to a time-varying flux linkage.

and i will be linear and we can define the *inductance* L as

$$L = \frac{\lambda}{i} \tag{1.28}$$

Substitution of Eqs. 1.5, 1.18 and 1.27 into Eq. 1.28 gives

$$L = \frac{N^2}{\mathcal{R}_{\text{tot}}} \tag{1.29}$$

from which we see that the inductance of a winding in a magnetic circuit is proportional to the square of the turns and inversely proportional to the reluctance of the magnetic circuit associated with that winding.

For example, from Eq. 1.20, under the assumption that the reluctance of the core is negligible as compared to that of the air gap, the inductance of the winding in Fig. 1.2 is equal to

$$L = \frac{N^2}{(g/\mu_0 A_g)} = \frac{N^2 \mu_0 A_g}{g} \tag{1.30}$$

Inductance is measured in *henrys* (H) or *weber-turns per ampere*. Equation 1.30 shows the dimensional form of expressions for inductance; inductance is proportional to the square of the number of turns, to a magnetic permeability and to a cross-sectional area and is inversely proportional to a length. It must be emphasized that strictly speaking, the concept of inductance requires a linear relationship between flux and mmf. Thus, it cannot be rigorously applied in situations where the non-linear characteristics of magnetic materials, as is discussed in Sections 1.3 and 1.4, dominate the performance of the magnetic system. However, in many situations of practical interest, the reluctance of the system is dominated by that of an air gap (which is of course linear) and the non-linear effects of the magnetic material can be ignored. In other cases it may be perfectly acceptable to assume an average value of magnetic permeability for the core material and to calculate a corresponding average inductance which can be used for calculations of reasonable engineering accuracy. Example 1.3 illustrates the former situation and Example 1.4 the latter.

EXAMPLE 1.3

The magnetic circuit of Fig. 1.6a consists of an N-turn winding on a magnetic core of infinite permeability with two parallel air gaps of lengths g_1 and g_2 and areas A_1 and A_2, respectively.

Find (a) the inductance of the winding and (b) the flux density B_1 in gap 1 when the winding is carrying a current i. Neglect fringing effects at the air gap.

Solution

a. The equivalent circuit of Fig. 1.6b shows that the total reluctance is equal to the parallel combination of the two gap reluctances. Thus

$$\phi = \frac{Ni}{\frac{\mathcal{R}_1 \mathcal{R}_2}{\mathcal{R}_1 + \mathcal{R}_2}}$$

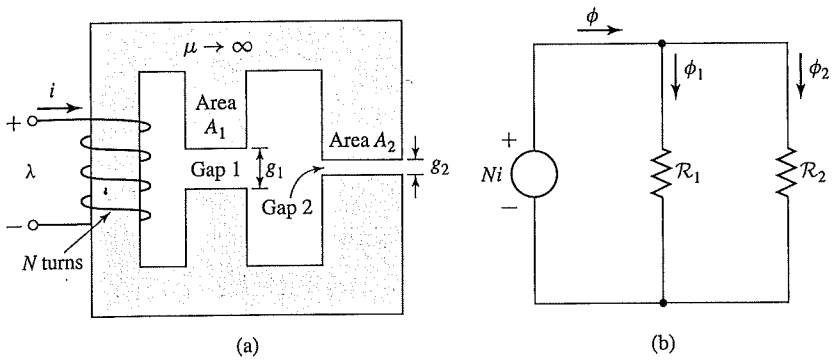

Figure 1.6 (a) Magnetic circuit and (b) equivalent circuit for Example 1.3.

where

$$\mathcal{R}_1 = \frac{g_1}{\mu_0 A_1} \qquad \mathcal{R}_2 = \frac{g_2}{\mu_0 A_2}$$

From Eq. 1.28,

$$L = \frac{\lambda}{i} = \frac{N\phi}{i} = \frac{N^2(\mathcal{R}_1 + \mathcal{R}_2)}{\mathcal{R}_1 \mathcal{R}_2}$$
$$= \mu_0 N^2 \left(\frac{A_1}{g_1} + \frac{A_2}{g_2} \right)$$

b. From the equivalent circuit, one can see that

$$\phi_1 = \frac{Ni}{\mathcal{R}_1} = \frac{\mu_0 A_1 Ni}{g_1}$$

and thus

$$B_1 = \frac{\phi_1}{A_1} = \frac{\mu_0 Ni}{g_1}$$

EXAMPLE 1.4

In Example 1.1, the relative permeability of the core material for the magnetic circuit of Fig. 1.2 is assumed to be $\mu_r = 70,000$ at a flux density of 1.0 T.

a. In a practical device, the core would be constructed from electrical steel such as M-5 electrical steel which is discussed in Section 1.3. This material is highly nonlinear and its relative permeability (defined for the purposes of this example as the ratio B/H) varies from a value of approximately $\mu_r = 72,300$ at a flux density of $B = 1.0$ T to a value of on the order of $\mu_r = 2,900$ as the flux density is raised to 1.8 T. Calculate the inductance under the assumption that the relative permeability of the core steel is 72,300.
b. Calculate the inductance under the assumption that the relative permeability is equal to 2,900.

Solution

a. From Eqs. 1.13 and 1.14 and based upon the dimensions given in Example 1.1,

$$\mathcal{R}_c = \frac{l_c}{\mu_r \mu_0 A_c} = \frac{0.3}{72{,}300\,(4\pi \times 10^{-7})(9 \times 10^{-4})} = 3.67 \times 10^3 \ \frac{\text{A} \cdot \text{turns}}{\text{Wb}}$$

while $\mathcal{R}_g$ remains unchanged from the value calculated in Example 1.1 as $\mathcal{R}_g = 4.42 \times 10^5$ A·turns/Wb.

Thus the total reluctance of the core and gap is

$$\mathcal{R}_{tot} = \mathcal{R}_c + \mathcal{R}_g = 4.46 \times 10^5 \ \frac{\text{A} \cdot \text{turns}}{\text{Wb}}$$

and hence from Eq. 1.29

$$L = \frac{N^2}{\mathcal{R}_{tot}} = \frac{500^2}{4.46 \times 10^5} = 0.561 \text{ H}$$

b. For $\mu_r = 2{,}900$, the reluctance of the core increases from a value of 3.79×10^3 A · turns / Wb to a value of

$$\mathcal{R}_c = \frac{l_c}{\mu_r \mu_0 A_c} = \frac{0.3}{2{,}900\,(4\pi \times 10^{-7})(9 \times 10^{-4})} = 9.15 \times 10^4 \ \frac{\text{A} \cdot \text{turns}}{\text{Wb}}$$

and hence the total reluctance increases from 4.46×10^5 A · turns / Wb to 5.34×10^5 A · turns / Wb. Thus from Eq. 1.29 the inductance decreases from 0.561 H to

$$L = \frac{N^2}{\mathcal{R}_{tot}} = \frac{500^2}{5.34 \times 10^5} = 0.468 \text{ H}$$

This example illustrates the linearizing effect of a dominating air gap in a magnetic circuit. In spite of a reduction in the permeablity of the iron by a factor of 72,300/2,900 = 25, the inductance decreases only by a factor of 0.468/0.561 = 0.83 simply because the reluctance of the air gap is significantly larger than that of the core. In many situations, it is common to assume the inductance to be constant at a value corresponding to a finite, constant value of core permeability (or in many cases it is assumed simply that $\mu_r \to \infty$). Analyses based upon such a representation for the inductor will often lead to results which are well within the range of acceptable engineering accuracy and which avoid the immense complication associated with modeling the non-linearity of the core material.

Practice Problem 1.3

Repeat the inductance calculation of Example 1.4 for a relative permeability $\mu_r = 30{,}000$.

Solution

$L = 0.554$ H

EXAMPLE 1.5

Using MATLAB,[6] plot the inductance of the magnetic circuit of Example 1.1 and Fig. 1.2 as a function of core permeability over the range $100 \leq \mu_r \leq 100{,}000$.

[6] "MATLAB" ia a registered trademarks of The MathWorks, Inc., 3 Apple Hill Drive, Natick, MA 01760, http://www.mathworks.com. A student edition of Matlab is available.

■ Solution

Here is the MATLAB script:

```
clc
clear

% Permeability of free space
mu0 = pi*4.e-7;

%All dimensions expressed in meters
Ac = 9e-4; Ag = 9e-4; g = 5e-4; lc = 0.3;
N = 500;

%Reluctance of air gap
Rg = g/(mu0*Ag);

mur = 1:100:100000;
Rc = lc./(mur*mu0*Ac);
Rtot = Rg+Rc;
L = N^2./Rtot;

plot(mur,L)
xlabel('Core relative permeability')
ylabel('Inductance [H]')
```

The resultant plot is shown in Fig. 1.7. Note that the figure clearly confirms that, for the magnetic circuit of this example, the inductance is quite insensitive to relative permeability

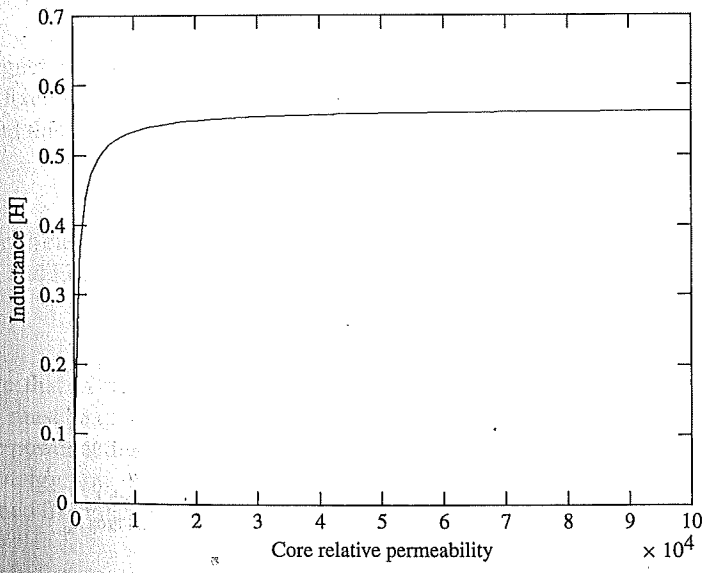

Figure 1.7 MATLAB plot of inductance vs. relative permeability for Example 1.5.

until the relative permeability drops to on the order of 1,000. Thus, as long as the effective relative permeability of the core is "large" (in this case greater than 1,000), any non-linearities in the properties of the core material will have little effect on the terminal properties of the inductor.

Practice Problem 1.4

Write a MATLAB script to plot the inductance of the magnetic circuit of Example 1.1 with $\mu_r = 70{,}000$ as a function of air-gap length as the the air gap is varied from 0.01 cm to 0.10 cm.

Figure 1.8 shows a magnetic circuit with an air gap and two windings. In this case note that the mmf acting on the magnetic circuit is given by the *total ampere-turns* acting on the magnetic circuit (i.e., the net ampere-turns of both windings) and that the reference directions for the currents have been chosen to produce flux in the same direction. The total mmf is therefore

$$\mathcal{F} = N_1 i_1 + N_2 i_2 \tag{1.31}$$

and from Eq. 1.20, with the reluctance of the core neglected and assuming that $A_c = A_g$, the core flux ϕ is

$$\phi = (N_1 i_1 + N_2 i_2)\frac{\mu_0 A_c}{g} \tag{1.32}$$

In Eq. 1.32, ϕ is the *resultant core flux* produced by the total mmf of the two windings. It is this resultant ϕ which determines the operating point of the core material.

If Eq. 1.32 is broken up into terms attributable to the individual currents, the resultant flux linkages of coil 1 can be expressed as

$$\lambda_1 = N_1\phi = N_1{}^2\left(\frac{\mu_0 A_c}{g}\right) i_1 + N_1 N_2\left(\frac{\mu_0 A_c}{g}\right) i_2 \tag{1.33}$$

which can be written

$$\lambda_1 = L_{11} i_1 + L_{12} i_2 \tag{1.34}$$

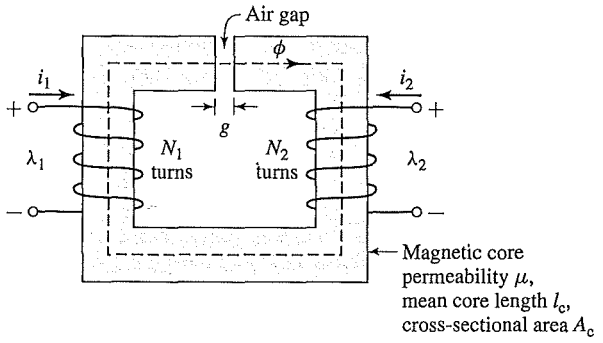

Figure 1.8 Magnetic circuit with two windings.

where

$$L_{11} = N_1{}^2 \frac{\mu_0 A_c}{g} \tag{1.35}$$

is the *self-inductance* of coil 1 and $L_{11}i_1$ is the flux linkage of coil 1 due to its own current i_1. The *mutual inductance* between coils 1 and 2 is

$$L_{12} = N_1 N_2 \frac{\mu_0 A_c}{g} \tag{1.36}$$

and $L_{12}i_2$ is the flux linkage of coil 1 due to current i_2 in the other coil. Similarly, the flux linkage of coil 2 is

$$\lambda_2 = N_2\phi = N_1 N_2 \left(\frac{\mu_0 A_c}{g}\right) i_1 + N_2{}^2 \left(\frac{\mu_0 A_c}{g}\right) i_2 \tag{1.37}$$

or

$$\lambda_2 = L_{21} i_1 + L_{22} i_2 \tag{1.38}$$

where $L_{21} = L_{12}$ is the mutual inductance and

$$L_{22} = N_2{}^2 \frac{\mu_0 A_c}{g} \tag{1.39}$$

is the self-inductance of coil 2.

It is important to note that the resolution of the resultant flux linkages into the components produced by i_1 and i_2 is based on superposition of the individual effects and therefore implies a linear flux-mmf relationship (characteristic of materials of constant permeability).

Substitution of Eq. 1.28 in Eq. 1.26 yields

$$e = \frac{d}{dt}(Li) \tag{1.40}$$

for a magnetic circuit with a single winding. For a static magnetic circuit, the inductance is fixed (assuming that material nonlinearities do not cause the inductance to vary), and this equation reduces to the familiar circuit-theory form

$$e = L\frac{di}{dt} \tag{1.41}$$

However, in electromechanical energy conversion devices, inductances are often time-varying, and Eq. 1.40 must be written as

$$e = L\frac{di}{dt} + i\frac{dL}{dt} \tag{1.42}$$

Note that in situations with multiple windings, the total flux linkage of each winding must be used in Eq. 1.26 to find the winding-terminal voltage.

The power at the terminals of a winding on a magnetic circuit is a measure of the rate of energy flow into the circuit through that particular winding. The *power*, p, is determined from the product of the voltage and the current

$$p = ie = i\frac{d\lambda}{dt} \tag{1.43}$$

and its unit is *watts* (W), or *joules per second*. Thus the change in *magnetic stored energy* ΔW in the magnetic circuit in the time interval t_1 to t_2 is

$$\Delta W = \int_{t_1}^{t_2} p\,dt = \int_{\lambda_1}^{\lambda_2} i\,d\lambda \tag{1.44}$$

In SI units, the magnetic stored energy W is measured in *joules* (J).

For a single-winding system of constant inductance, the change in magnetic stored energy as the flux level is changed from λ_1 to λ_2 can be written as

$$\Delta W = \int_{\lambda_1}^{\lambda_2} i\,d\lambda = \int_{\lambda_1}^{\lambda_2} \frac{\lambda}{L}\,d\lambda = \frac{1}{2L}(\lambda_2^2 - \lambda_1^2) \tag{1.45}$$

The total magnetic stored energy at any given value of λ can be found from setting λ_1 equal to zero:

$$W = \frac{1}{2L}\lambda^2 = \frac{L}{2}i^2 \tag{1.46}$$

EXAMPLE 1.6

For the magnetic circuit of Example 1.1 (Fig. 1.2), find (a) the inductance L, (b) the magnetic stored energy W for $B_c = 1.0$ T, and (c) the induced voltage e for a 60-Hz time-varying core flux of the form $B_c = 1.0 \sin \omega t$ T where $\omega = (2\pi)(60) = 377$.

■ Solution

a. From Eqs. 1.16 and 1.28 and Example 1.1,

$$L = \frac{\lambda}{i} = \frac{N\phi}{i} = \frac{N^2}{\mathcal{R}_c + \mathcal{R}_g}$$

$$= \frac{500^2}{4.46 \times 10^5} = 0.56\,\text{H}$$

Note that the core reluctance is much smaller than that of the gap ($\mathcal{R}_c \ll \mathcal{R}_g$). Thus to a good approximation the inductance is dominated by the gap reluctance, i.e.,

$$L \approx \frac{N^2}{\mathcal{R}_g} = 0.57\,\text{H}$$

b. In Example 1.1 we found that when $B_c = 1.0$ T, $i = 0.80$ A. Thus from Eq. 1.46,

$$W = \frac{1}{2}Li^2 = \frac{1}{2}(0.56)(0.80)^2 = 0.18\,\text{J}$$

c. From Eq. 1.26 and Example 1.1,

$$e = \frac{d\lambda}{dt} = N\frac{d\varphi}{dt} = NA_c\frac{dB_c}{dt}$$

$$= 500 \times (9 \times 10^{-4}) \times (377 \times 1.0\cos(377t))$$

$$= 170\cos(377t) \quad V$$

Practice Problem 1.5

Repeat Example 1.6 for $B_c = 0.8$ T and assuming the core flux varies at 50 Hz instead of 60 Hz.

Solution

a. The inductance L is unchanged.
b. $W = 0.115$ J
c. $e = 113 \cos(314t)$ V

1.3 PROPERTIES OF MAGNETIC MATERIALS

In the context of electromechanical-energy-conversion devices, the importance of magnetic materials is twofold. Through their use it is possible to obtain large magnetic flux densities with relatively low levels of magnetizing force. Since magnetic forces and energy density increase with increasing flux density, this effect plays a large role in the performance of energy-conversion devices.

In addition, magnetic materials can be used to constrain and direct magnetic fields in well-defined paths. In a transformer they are used to maximize the coupling between the windings as well as to lower the excitation current required for transformer operation. In electric machinery magnetic materials are used to shape the fields to obtain desired torque-production and electrical terminal characteristics. Thus a knowledgeable designer can use magnetic materials to achieve specific desirable device characteristics.

Ferromagnetic materials, typically composed of iron and alloys of iron with cobalt, tungsten, nickel, aluminum, and other metals, are by far the most common magnetic materials. Although these materials are characterized by a wide range of properties, the basic phenomena responsible for their properties are common to them all.

Ferromagnetic materials are found to be composed of a large number of domains, i.e., regions in which the magnetic moments of all the atoms are parallel, giving rise to a net magnetic moment for that domain. In an unmagnetized sample of material, the domain magnetic moments are randomly oriented, and the net resulting magnetic flux in the material is zero.

When an external magnetizing force is applied to this material, the domain magnetic moments tend to align with the applied magnetic field. As a result, the domain magnetic moments add to the applied field, producing a much larger value of flux density than would exist due to the magnetizing force alone. Thus the *effective permeability* μ, equal to the ratio of the total magnetic flux density to the applied magnetic-field intensity, is large compared with the permeability of free space μ_0. As the magnetizing force is increased, this behavior continues until all the magnetic moments are aligned with the applied field; at this point they can no longer contribute to increasing the magnetic flux density, and the material is said to be fully *saturated*.

In the absence of an externally applied magnetizing force, the domain magnetic moments naturally align along certain directions associated with the crystal structure of the domain, known as axes of easy magnetization. Thus if the applied magnetizing

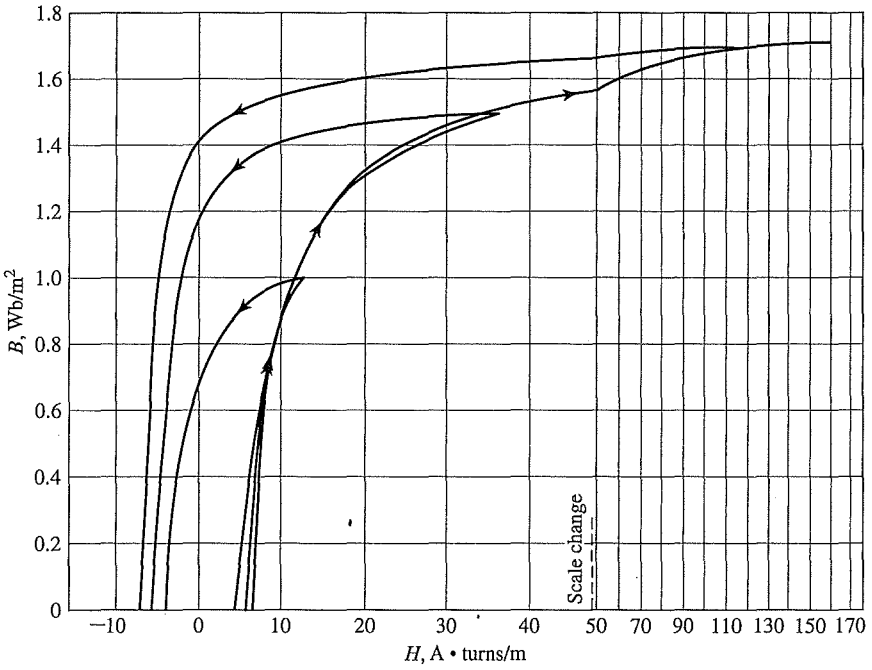

Figure 1.9 *B-H* loops for M-5 grain-oriented electrical steel 0.012 in thick. Only the top halves of the loops are shown here. (Armco Inc)

force is reduced, the domain magnetic moments relax to the direction of easy magnetism nearest to that of the applied field. As a result, when the applied field is reduced to zero, although they will tend to relax towards their initial orientation, the magnetic dipole moments will no longer be totally random in their orientation; they will retain a net magnetization component along the applied field direction. It is this effect which is responsible for the phenomenon known as *magnetic hysteresis*.

Due to this hysteresis effect, the relationship between B and H for a ferromagnetic material is both nonlinear and multivalued. In general, the characteristics of the material cannot be described analytically. They are commonly presented in graphical form as a set of empirically determined curves based on test samples of the material using methods prescribed by the American Society for Testing and Materials (ASTM).[7]

The most common curve used to describe a magnetic material is the *B-H curve* or *hysteresis loop*. The first and second quadrants (corresponding to $B \geq 0$) of a set of hysteresis loops are shown in Fig. 1.9 for M-5 steel, a typical grain-oriented

[7] Numerical data on a wide variety of magnetic materials are available from material manufacturers. One problem in using such data arises from the various systems of units employed. For example, magnetization may be given in oersteds or in ampere-turns per meter and the magnetic flux density in gauss, kilogauss, or teslas. A few useful conversion factors are given in Appendix D. The reader is reminded that the equations in this book are based upon SI units.

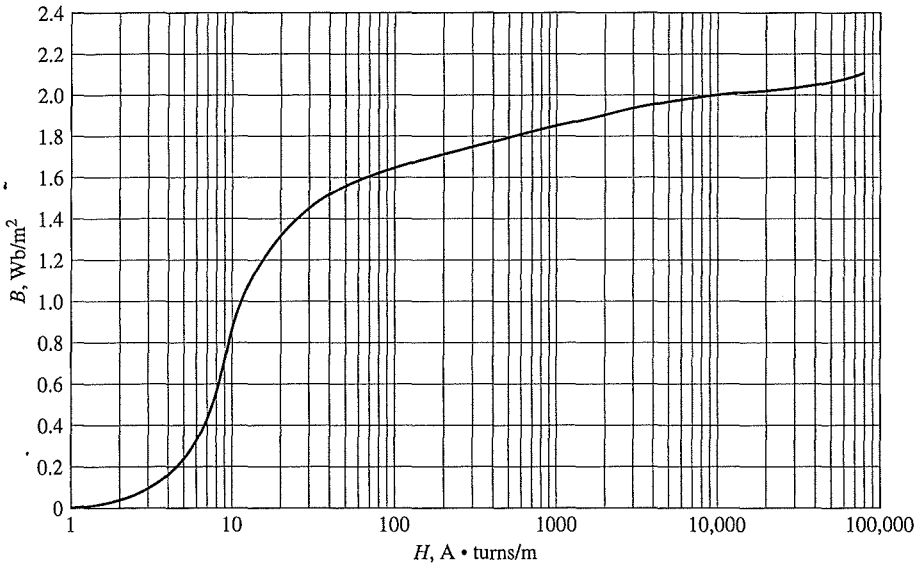

Figure 1.10 Dc magnetization curve for M-5 grain-oriented electrical steel 0.012 in. thick. (Armco Inc.)

electrical steel used in electric equipment. These loops show the relationship between the magnetic flux density B and the magnetizing force H. Each curve is obtained while cyclically varying the applied magnetizing force between equal positive and negative values of fixed magnitude. Hysteresis causes these curves to be multivalued. After several cycles the B-H curves form closed loops as shown. The arrows show the paths followed by B with increasing and decreasing H. Notice that with increasing magnitude of H the curves begin to flatten out as the material tends toward saturation. At a flux density of about 1.7 T this material can be seen to be heavily saturated.

Notice also that as H is decreased from its maximum value to zero, the flux density decreases but not to zero. This is the result of the relaxation of the orientation of the magnetic moments of the domains as described above. The result is that there remains a *remanent magnetization* when H is zero.

Fortunately, for many engineering applications, it is sufficient to describe the material by a single-valued curve obtained by plotting the locus of the maximum values of B and H at the tips of the hysteresis loops; this is known as a *dc* or *normal magnetization curve*. A dc magnetization curve for M-5 grain-oriented electrical steel is shown in Fig. 1.10. The dc magnetization curve neglects the hysteretic nature of the material but clearly displays its nonlinear characteristics.

EXAMPLE 1.7

Assume that the core material in Example 1.1 is M-5 electrical steel, which has the dc magnetization curve of Fig. 1.10. Find the current i required to produce $B_c = 1$ T.

■ Solution

The value of H_c for $B_c = 1$ T is read from Fig. 1.10 as

$$H_c = 11 \text{ A} \cdot \text{turns/m}$$

The mmf drop for the core path is

$$\mathcal{F}_c = H_c l_c = 11(0.3) = 3.3 \text{ A} \cdot \text{turns}$$

Neglecting fringing, $B_g = B_c$ and the mmf drop across the air gap is

$$\mathcal{F}_g = H_g g = \frac{B_g g}{\mu_0} = \frac{1(5 \times 10^{-4})}{4\pi \times 10^{-7}} = 396 \text{ A} \cdot \text{turns}$$

The required current is

$$i = \frac{\mathcal{F}_c + \mathcal{F}_g}{N} = \frac{399}{500} = 0.80 \text{ A}$$

Practice Problem 1.6

Repeat Example 1.7 but find the current i for $B_c = 1.6$ T. By what factor does the current have to be increased to result in this factor of 1.6 increase in flux density?

Solution

The current i can be shown to be 1.302 A. Thus, the current must be increased by a factor of 1.302/0.8 = 1.63. Because of the dominance of the air-gap reluctance, this is just slightly in excess of the fractional increase in flux density in spite of the fact that the core is beginning to significantly saturate at a flux density of 1.6 T.

1.4 AC EXCITATION

In ac power systems, the waveforms of voltage and flux closely approximate sinusoidal functions of time. This section describes the excitation characteristics and losses associated with steady-state ac operation of magnetic materials under such operating conditions. We use as our model a closed-core magnetic circuit, i.e., with no air gap, such as that shown in Fig. 1.1. The magnetic path length is l_c, and the cross-sectional area is A_c throughout the length of the core. We further assume a sinusoidal variation of the core flux $\varphi(t)$; thus

$$\varphi(t) = \phi_{max} \sin \omega t = A_c B_{max} \sin \omega t \tag{1.47}$$

where

ϕ_{max} = amplitude of core flux φ in webers
B_{max} = amplitude of flux density B_c in teslas
ω = angular frequency = $2\pi f$
f = frequency in Hz

From Eq. 1.26, the voltage induced in the N-turn winding is

$$e(t) = \omega N \phi_{max} \cos(\omega t) = E_{max} \cos \omega t \tag{1.48}$$

where

$$E_{max} = \omega N \phi_{max} = 2\pi f N A_c B_{max} \tag{1.49}$$

In steady-state ac operation, we are usually more interested in the *root-mean-square* or *rms* values of voltages and currents than in instantaneous or maximum values. In general, the rms value of a periodic function of time, $f(t)$, of period T is defined as

$$F_{rms} = \sqrt{\left(\frac{1}{T}\int_0^T f^2(t)\,dt\right)} \tag{1.50}$$

From Eq. 1.50, the rms value of a sine wave can be shown to be $1/\sqrt{2}$ times its peak value. Thus the rms value of the induced voltage is

$$E_{rms} = \frac{2\pi}{\sqrt{2}} f N A_c B_{max} = \sqrt{2}\,\pi f N A_c B_{max} \tag{1.51}$$

An *excitation current* i_φ, corresponding to an excitation mmf $Ni_\varphi(t)$, is required to produce the flux $\varphi(t)$ in the core.[8] Because of the nonlinear magnetic properties of the core, the excitation current corresponding to a sinusoidal core flux will be non sinusoidal. A curve of the exciting current as a function of time can be found graphically from the magnetic characteristics of the core material, as illustrated in Fig. 1.11a. Since B_c and H_c are related to φ and i_φ by known geometric constants, the ac hysteresis loop of Fig. 1.11b has been drawn in terms of $\varphi = B_c A_c$ and is $i_\varphi = H_c l_c / N$. Sine waves of induced voltage, e, and flux, φ, in accordance with Eqs. 1.47 and 1.48, are shown in Fig. 1.11a.

At any given time, the value of i_φ corresponding to the given value of flux can be found directly from the hysteresis loop. For example, at time t' the flux is φ' and the current is i'_φ; at time t'' the corresponding values are φ'' and i''_φ. Notice that since the hysteresis loop is multivalued, it is necessary to be careful to pick the rising-flux values (φ' in the figure) from the rising-flux portion of the hysteresis loop; similarly the falling-flux portion of the hysteresis loop must be selected for the falling-flux values (φ'' in the figure).

Notice that, because the hysteresis loop "flattens out" due to saturation effects, the waveform of the exciting current is sharply peaked. Its rms value $I_{\varphi,rms}$ is defined by Eq. 1.50, where T is the period of a cycle. It is related to the corresponding rms value H_{rms} of H_c by the relationship

$$I_{\varphi,rms} = \frac{l_c H_{rms}}{N} \tag{1.52}$$

The ac excitation characteristics of core materials are often described in terms of rms voltamperes rather than a magnetization curve relating B and H. The theory

[8] More generally, for a system with multiple windings, the exciting mmf is the net ampere-turns acting to produce flux in the magnetic circuit.

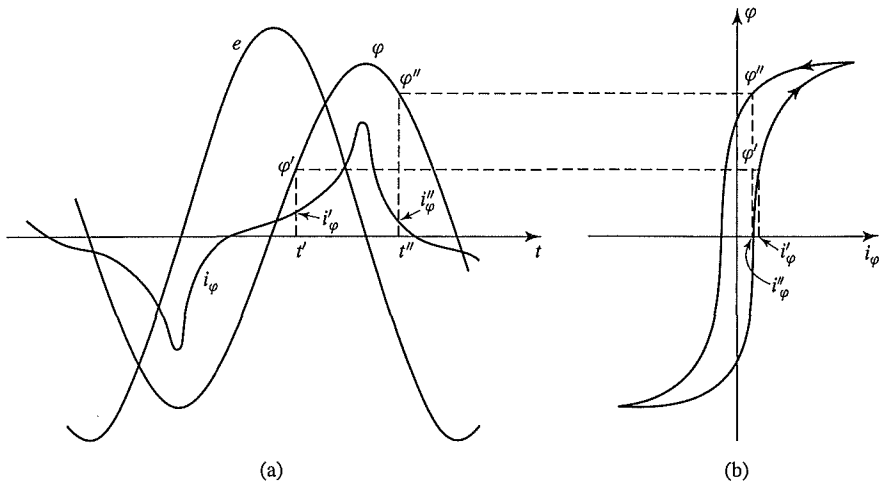

Figure 1.11 Excitation phenomena. (a) Voltage, flux, and exciting current; (b) corresponding hysteresis loop.

behind this representation can be explained by combining Eqs. 1.51 and 1.52. From Eqs. 1.51 and 1.52, the rms voltamperes required to excite the core of Fig. 1.1 to a specified flux density is equal to

$$E_{\text{rms}} I_{\varphi,\text{rms}} = \sqrt{2}\,\pi f N A_c B_{\max} \frac{l_c H_{\text{rms}}}{N}$$
$$= \sqrt{2}\,\pi f B_{\max} H_{\text{rms}} (A_c l_c) \tag{1.53}$$

In Eq. 1.53, the product $A_c l_c$ can be seen to be equal to the volume of the core and hence the rms exciting voltamperes required to excite the core with sinusoidal can be seen to be proportional to the frequency of excitation, the core volume and the product of the peak flux density, and the rms magnetic field intensity. For a magnetic material of mass density ρ_c, the mass of the core is $A_c l_c \rho_c$ and the *exciting rms voltamperes per unit mass*, S_a, can be expressed as

$$S_a = \frac{E_{\text{rms}} I_{\varphi,\text{rms}}}{\text{mass}} = \sqrt{2}\,\pi f \left(\frac{B_{\max} H_{\text{rms}}}{\rho_c} \right) \tag{1.54}$$

Note that, normalized in this fashion, the rms exciting voltamperes depends only on the frequency and $B_{\max}$ because H_{rms} is a unique function of $B_{\max}$ as determined by the shape of the material hysteresis loop at any given frequency f. As a result, the ac excitation requirements for a magnetic material are often supplied by manufacturers in terms of rms voltamperes per unit mass as determined by laboratory tests on closed-core samples of the material. These results are illustrated in Fig. 1.12 for M-5 grain-oriented electrical steel.

The exciting current supplies the mmf required to produce the core flux and the power input associated with the energy in the magnetic field in the core. Part of this

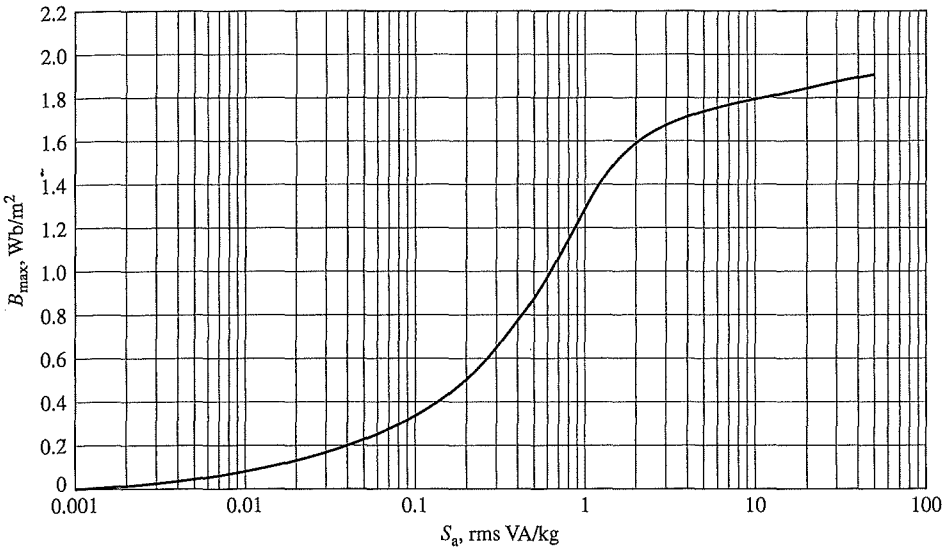

Figure 1.12 Exciting rms voltamperes per kilogram at 60 Hz for M-5 grain-oriented electrical steel 0.012 in. thick. (Armco Inc.)

energy is dissipated as losses and results in heating of the core. The rest appears as reactive power associated with energy storage in the magnetic field. This reactive power is not dissipated in the core; it is cyclically supplied and absorbed by the excitation source.

Two loss mechanisms are associated with time-varying fluxes in magnetic materials. The first is due to the hysteretic nature of magnetic material. As has been discussed, in a magnetic circuit like that of Fig. 1.1, a time-varying excitation will cause the magnetic material to undergo a cyclic variation described by a hysteresis loop such as that shown in Fig. 1.13.

Equation 1.44 can be used to calculate the energy input W to the magnetic core of Fig. 1.1 as the material undergoes a single cycle

$$W = \oint i_\varphi \, d\lambda = \oint \left(\frac{H_c l_c}{N}\right)(A_c N \, dB_c) = A_c l_c \oint H_c \, dB_c \qquad (1.55)$$

Recognizing that $A_c l_c$ is the volume of the core and that the integral is the area of the ac hysteresis loop, we see that each time the magnetic material undergoes a cycle, there is a net energy input into the material. This energy is required to move around the magnetic dipoles in the material and is dissipated as heat in the material. Thus for a given flux level, the corresponding *hysteresis losses* are proportional to the area of the hysteresis loop and to the total volume of material. Since there is an energy loss per cycle, hysteresis power loss is proportional to the frequency of the applied excitation.

The second loss mechanism is ohmic heating, associated with induced currents in the core material. From Faraday's law (Eq. 1.25) we see that time-varying magnetic

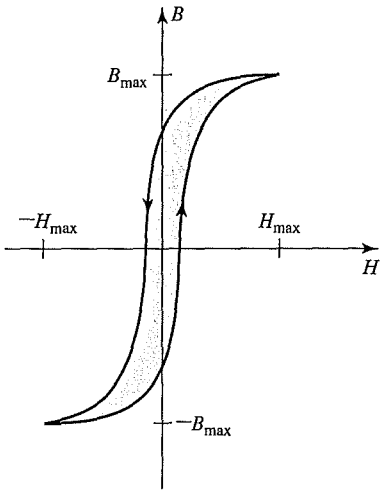

Figure 1.13 Hysteresis loop; hysteresis loss is proportional to the loop area (shaded).

fields give rise to electric fields. In magnetic materials these electric fields result in induced currents, commonly referred to as *eddy currents*, which circulate in the core material and oppose changes in flux density in the material. To counteract the corresponding demagnetizing effect, the current in the exciting winding must increase. Thus the resultant "dynamic" *B-H* loop under ac operation is somewhat "fatter" than the hysteresis loop for slowly varying conditions and this effect increases as the excitation frequency is increased. It is for this reason that the charactersitics of electrical steels vary with frequency and hence manufacturers typically supply characteristics over the expected operating frequency range of a particular electrical steel. Note for example that the exciting rms voltamperes of Fig. 1.12 are specified at a frequency of 60 Hz.

To reduce the effects of eddy currents, magnetic structures are usually built with thin sheets or *laminations* of magnetic material. These laminations, which are aligned in the direction of the field lines, are insulated from each other by an oxide layer on their surfaces or by a thin coat of insulating enamel or varnish. This greatly reduces the magnitude of the eddy currents since the layers of insulation interrupt the current paths; the thinner the laminations, the lower the losses. In general, as a first approximation, eddy-current loss can be considered to increase as the square of the excitation frequency and also as the square of the peak flux density.

In general, core losses depend on the metallurgy of the material as well as the flux density and frequency. Information on core loss is typically presented in graphical form. It is plotted in terms of watts per unit mass as a function of flux density; often a family of curves for different frequencies is given. Figure 1.14 shows the core loss density P_c for M-5 grain-oriented electrical steel at 60 Hz.

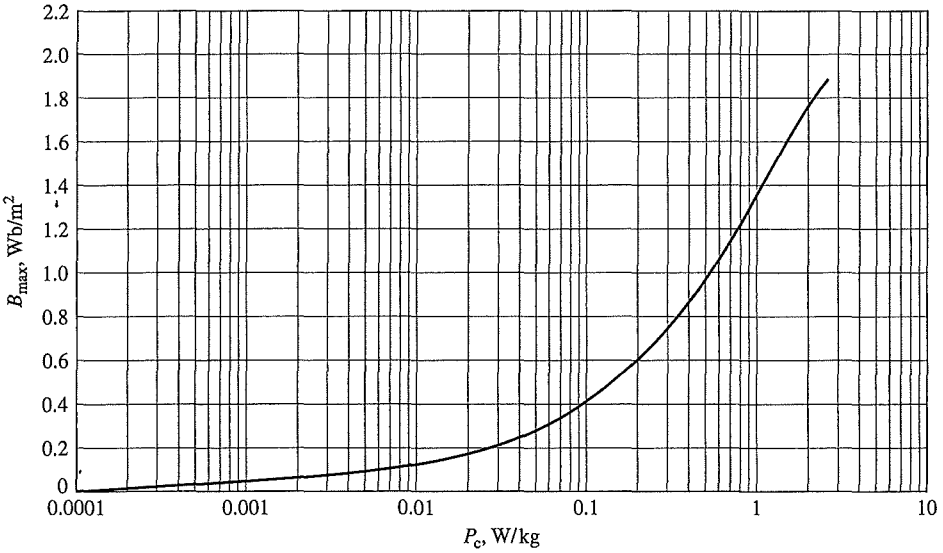

Figure 1.14 Core loss density at 60 Hz in watts per kilogram for M-5 grain-oriented electrical steel 0.012 in. thick. (Armco Inc.)

Nearly all transformers and certain components of electric machines use sheet-steel material that has highly favorable directions of magnetization along which the core loss is low and the permeability is high. This material is termed *grain-oriented steel.* The reason for this property lies in the atomic structure of a crystal of the silicon-iron alloy, which is a body-centered cube; each cube has an atom at each corner as well as one in the center of the cube. In the cube, the easiest axis of magnetization is the cube edge; the diagonal across the cube face is more difficult, and the diagonal through the cube is the most difficult. By suitable manufacturing techniques most of the crystalline cube edges are aligned in the rolling direction to make it the favorable direction of magnetization. The behavior in this direction is superior in core loss and permeability to *nonoriented steels* in which the crystals are randomly oriented to produce a material with characteristics which are uniform in all directions. As a result, oriented steels can be operated at higher flux densities than the nonoriented grades.

Nonoriented electrical steels are used in applications where the flux does not follow a path which can be oriented with the rolling direction or where low cost is of importance. In these steels the losses are somewhat higher and the permeability is very much lower than in grain-oriented steels.

EXAMPLE 1.8

The magnetic core in Fig. 1.15 is made from laminations of M-5 grain-oriented electrical steel. The winding is excited with a 60-Hz voltage to produce a flux density in the steel of $B = 1.5 \sin \omega t$ T, where $\omega = 2\pi 60 \approx 377$ rad/sec. The steel occupies 0.94 of the core cross-sectional area. The mass-density of the steel is 7.65 g/cm^3. Find (a) the applied voltage, (b) the peak current, (c) the rms exciting current, and (d) the core loss.

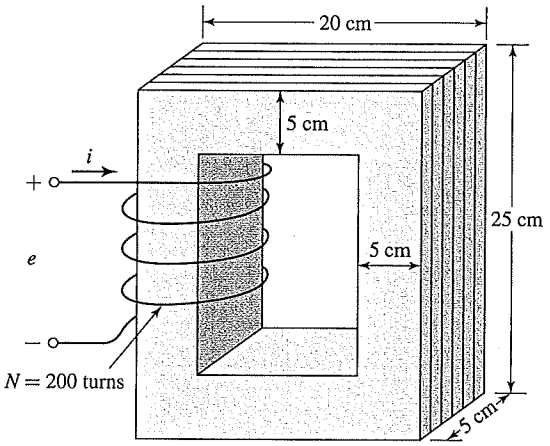

Figure 1.15 Laminated steel core with winding for Example 1.8.

■ Solution

a. From Eq. 1.26 the voltage is

$$\begin{aligned} e &= N\frac{d\varphi}{dt} = NA_c\frac{dB}{dt} \\ &= 200 \times 25\ \text{cm}^2 \times 0.94 \times 1.5 \times 377\ \cos(377t) \\ &= 266\cos(377t)\ \text{V} \end{aligned}$$

b. The magnetic field intensity corresponding to $B_{max} = 1.5$ T is given in Fig. 1.10 as $H_{max} = 36$ A turns/m. Notice that, as expected, the relative permeability $\mu_r = B_{max}/(\mu_0 H_{max}) = 33{,}000$ at the flux level of 1.5 T is lower than the value of $\mu_r = 72{,}300$ found in Example 1.4 corresponding to a flux level of 1.0 T, yet significantly larger than the value of 2,900 corresponding to a flux level of 1.8 T.

$$l_c = (15 + 15 + 20 + 20)\ \text{cm} = 0.70\ \text{m}$$

The peak current is

$$I = \frac{H_{max} l_c}{N} = \frac{36 \times 0.70}{200} = 0.13\ \text{A}$$

c. The rms current is obtained from the value of S_a of Fig. 1.12 for $B_{max} = 1.5$ T.

$$S_a = 1.5\ \text{VA/kg}$$

The core volume and mass are

$$\text{Vol}_c = 25\ \text{cm}^2 \times 0.94 \times 70\ \text{cm} = 1645\ \text{cm}^3$$

$$M_c = 1645\ \text{cm}^3 \times \left(\frac{7.65\ \text{g}}{1.0\ \text{cm}^3}\right) = 12.6\ \text{kg}$$

The total rms voltamperes and current are

$$S = 1.5 \text{ VA/kg} \times 12.6 \text{ kg} = 18.9 \text{ VA}$$

$$I_{\varphi,\text{rms}} = \frac{S}{E_{\text{rms}}} = \frac{18.9}{266/\sqrt{2}} = 0.10 \text{ A}$$

d. The core-loss density is obtained from Fig. 1.14 as $P_c = 1.2$ W/kg. The total core loss is

$$P_{\text{core}} = 1.2 \text{ W/kg} \times 12.6 \text{ kg} = 15.1 \text{ W}$$

Practice Problem 1.7

Repeat Example 1.8 for a 60-Hz voltage of $B = 1.0 \sin \omega t$ T.

Solution

a. $V = 177 \cos 377t$ V
b. $I = 0.042$ A
c. $I_\varphi = 0.041$ A
d. $P = 6.5$ W

1.5 PERMANENT MAGNETS

Figure 1.16a shows the second quadrant of a hysteresis loop for Alnico 5, a typical permanent-magnet material, while Fig. 1.16b shows the second quadrant of a hysteresis loop for M-5 steel.[9] Notice that the curves are similar in nature. However, the hysteresis loop of Alnico 5 is characterized by a large value of *residual* or *remanent magnetization*, B_r, (approximately 1.22 T) as well as a large value of *coercivity*, H_c, (approximately −49 kA/m).

The residual magnetization, B_r, corresponds to the flux density which would remain in a section of the material if the applied mmf (and hence the magnetic field intensity H) were reduced to zero. However, although the M-5 electrical steel also has a large value of residual magnetization (approximately 1.4 T), it has a much smaller value of coercivity (approximately -6 A/m, smaller by a factor of over 7500). The coercivity H_c is the value of magnetic field intensity (which is proportional to the mmf) required to reduce the material flux density to zero. As we will see, the lower the coercivity of a given magnetic material, the easier it is to demagnetize it.

The significance of residual magnetization is that it can produce magnetic flux in a magnetic circuit in the absence of external excitation such as is produced by winding currents. This is a familiar phenomenon to anyone who has afixed notes to a refrigerator with small magnets and is widely used in devices such as loudspeakers and permanent-magnet motors.

[9] To obtain the largest value of residual magnetization, the hysteresis loops of Fig. 1.16 are those which would be obtained if the materials were excited by sufficient mmf to ensure that they were driven heavily into saturation. This is discussed further in Section 1.6.

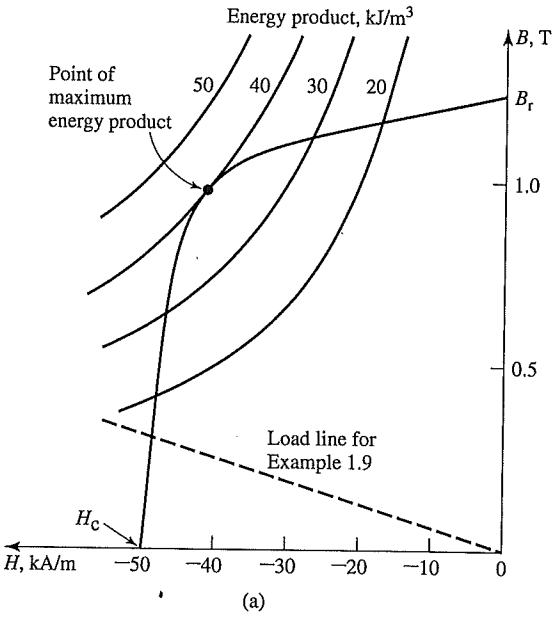

(a)

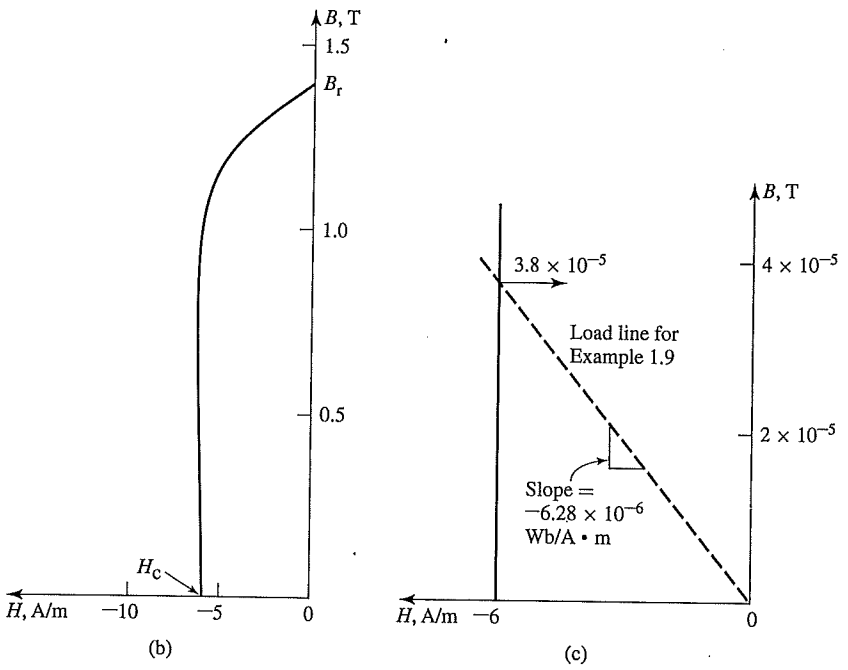

(b) (c)

Figure 1.16 (a) Second quadrant of hysteresis loop for Alnico 5; (b) second quadrant of hysteresis loop for M-5 electrical steel; (c) hysteresis loop for M-5 electrical steel expanded for small *B*. (Armco Inc.)

From Fig. 1.16, it would appear that both Alnico 5 and M-5 electrical steel would be useful in producing flux in unexcited magnetic circuits since they both have large values of residual magnetization. That this is not the case can be best illustrated by an example.

EXAMPLE 1.9

As shown in Fig. 1.17, a magnetic circuit consists of a core of high permeability ($\mu \rightarrow \infty$), an air gap of length $g = 0.2$ cm, and a section of magnetic material of length $l_m = 1.0$ cm. The cross-sectional area of the core and gap is equal to $A_m = A_g = 4$ cm^2. Calculate the flux density B_g in the air gap if the magnetic material is (a) Alnico 5 and (b) M-5 electrical steel.

Solution

a. Since the core permeability is assumed infinite, H in the core is negligible (otherwise a finite H would produce an infinite B). Recognizing that there is zero mmf acting on the magnetic circuit of Fig. 1.17, we can write

$$\mathcal{F} = 0 = H_g g + H_m l_m$$

or

$$H_g = -\left(\frac{l_m}{g}\right) H_m$$

where H_g and H_m are the magnetic field intensities in the air gap and the magnetic material, respectively.

Since the flux must be continuous through the magnetic circuit,

$$\phi = A_g B_g = A_m B_m$$

or

$$B_g = \left(\frac{A_m}{A_g}\right) B_m$$

where B_g and B_m are the magnetic flux densities in the air gap and the magnetic material, respectively.

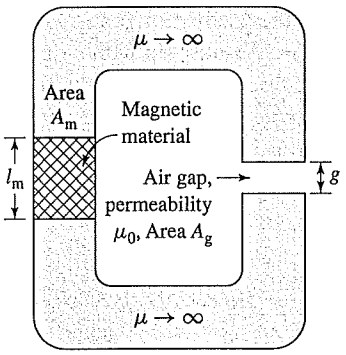

Figure 1.17 Magnetic circuit for Example 1.9.

These equations can be solved to yield a linear relationship for B_m in terms of H_m

$$B_m = -\mu_0 \left(\frac{A_g}{A_m}\right)\left(\frac{l_m}{g}\right) H_m = -5\,\mu_0\, H_m = -6.28 \times 10^{-6} H_m$$

To solve for B_m we recognize that for Alnico 5, B_m and H_m are also related by the curve of Fig. 1.16a. Thus this linear relationship, commonly referred to as a *load line*, can be plotted on Fig. 1.16a and the solution obtained graphically, resulting in

$$B_g = B_m = 0.30\ \text{T} = 3{,}000\ \text{gauss}$$

b. The solution for M-5 electrical steel proceeds exactly as in part (a). The load line is the same as that of part (a) because it is determined only by the permeability of the air gap and the geometries of the magnet and the air gap. Hence from Fig. 1.16c

$$B_g = 3.8 \times 10^{-5}\ \text{T} = 0.38\ \text{gauss}$$

which is much less than the value obtained with Alnico 5 and is essentially negligible.

Example 1.9 shows that there is an immense difference between permanent-magnet materials (often referred to as *hard magnetic materials*) such as Alnico 5 and *soft magnetic materials* such as M-5 electrical steel. This difference is characterized in large part by the immense difference in their coercivities H_c. The coercivity is a measure of the magnitude of the mmf required to reduce the material flux density to zero. As seen from Example 1.9, it is also a measure of the capability of the material to produce flux in a magnetic circuit which includes an air gap. Thus we see that materials which make good permanent magnets are characterized by large values of coercivity H_c (considerably in excess of 1 kA/m).

A useful measure of the capability of permanent-magnet material is known as its *maximum energy product*. This corresponds to the largest magnitude of the B-H product $(B \cdot H)_{max}$ found in the second quadrant of that material's hysteresis loop. As can be seen from Eq. 1.55, the product of B and H has the dimensions of energy density (joules per cubic meter). We now show that operation of a given permanent-magnet material in a magnetic circuit at this point will result in the smallest volume of that material required to produce a given flux density in an air gap.

In Example 1.9, we found an expression for the flux density in the air gap of the magnetic circuit of Fig. 1.17:

$$B_g = \frac{A_m}{A_g} B_m \tag{1.56}$$

We also found that

$$H_g = -\left(\frac{l_m}{g}\right) H_m \tag{1.57}$$

Equation 1.57 can be multiplied by μ_0 to obtain $B_g = \mu_0 H_g$. Multiplying by Eq. 1.56 yields

$$B_g^2 = \mu_0 \left(\frac{l_m A_m}{g A_g} \right) (-H_m B_m)$$

$$= \mu_0 \left(\frac{\text{Vol}_{\text{mag}}}{\text{Vol}_{\text{air gap}}} \right) (-H_m B_m) \tag{1.58}$$

where Vol_{mag} is the volume of the magnet, $\text{Vol}_{\text{air gap}}$ is the air-gap volume, and the minus sign arises because, at the operating point of the magnetic circuit, H in the magnet (H_m) is negative.

Solving Eq. 1.58 gives

$$\text{Vol}_{\text{mag}} = \frac{\text{Vol}_{\text{air gap}} B_g^2}{\mu_0 (-H_m B_m)} \tag{1.59}$$

which is the desired result. It indicates that to achieve a desired flux density in the air gap, the required volume of the magnet can be minimized by operating the magnet at the point of the largest possible value of the B-H product $H_m B_m$, i.e., at the point of maximum energy product. Furthermore, the larger the value of this product, the smaller the size of the magnet required to produce the desired flux density. Hence the maximum energy product is a useful performance measure for a magnetic material and it is often found as a tabulated "figure of merit" on data sheets for permanent-magnet materials. As a practical matter, this result applies to many practical engineering applications where the use of a permanent-magnet material with the largest available maximum energy product will result in the smallest required magnet volume.

Equation 1.58 appears to indicate that one can achieve an arbitrarily large air-gap flux density simply by reducing the air-gap volume. This is not true in practice because a reduction in air-gap length will increase the flux density in the magnetic circuit and as the flux density in the magnetic circuit increases, a point will be reached at which the magnetic core material will begin to saturate and the assumption of infinite permeability will no longer be valid, thus invalidating the derivation leading to Eq. 1.58.

EXAMPLE 1.10

The magnetic circuit of Fig. 1.17 is modified so that the air-gap area is reduced to $A_g = 2.0\,\text{cm}^2$, as shown in Fig. 1.18. Find the minimum magnet volume required to achieve an air-gap flux density of 0.8 T.

■ Solution

Note that a curve of constant B-H product is a hyperbola. A set of such hyperbolas for different values of the B-H product is plotted in Fig. 1.16a. From these curves, we see that the maximum energy product for Alnico 5 is 40 kJ/m^3 and that this occurs at the point $B = 1.0$ T and $H = -40$ kA/m. The smallest magnet volume will be achieved with the magnet operating at this point.

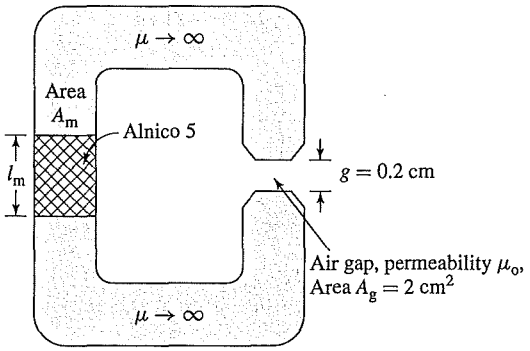

Figure 1.18 Magnetic circuit for Example 1.10.

Thus from Eq. 1.56,

$$A_m = A_g \left(\frac{B_g}{B_m}\right)$$

$$= 2 \text{ cm}^2 \left(\frac{0.8}{1.0}\right) = 1.6 \text{ cm}^2$$

and from Eq. 1.57

$$l_m = -g\left(\frac{H_g}{H_m}\right) = -g\left(\frac{B_g}{\mu_0 H_m}\right)$$

$$= -0.2 \text{ cm} \left(\frac{0.8}{(4\pi \times 10^{-7})(-40 \times 10^3)}\right)$$

$$= 3.18 \text{ cm}$$

Thus the minimum magnet volume is equal to $1.6 \text{ cm}^2 \times 3.18 \text{ cm} = 5.09 \text{ cm}^3$.

Practice Problem 1.8

Repeat Example 1.10 assuming the air-gap area is further reduced to $A_g = 1.8 \text{ cm}^2$ and that the desired air-gap flux density is 0.6 T.

Solution

Minimum magnet volume = 2.58 cm^3.

1.6 APPLICATION OF PERMANENT-MAGNET MATERIALS

Examples 1.9 and 1.10 consider the operation of permanent-magnetic materials under the assumption that the operating point can be determined simply from a knowledge of the geometry of the magnetic circuit and the properties of the various magnetic

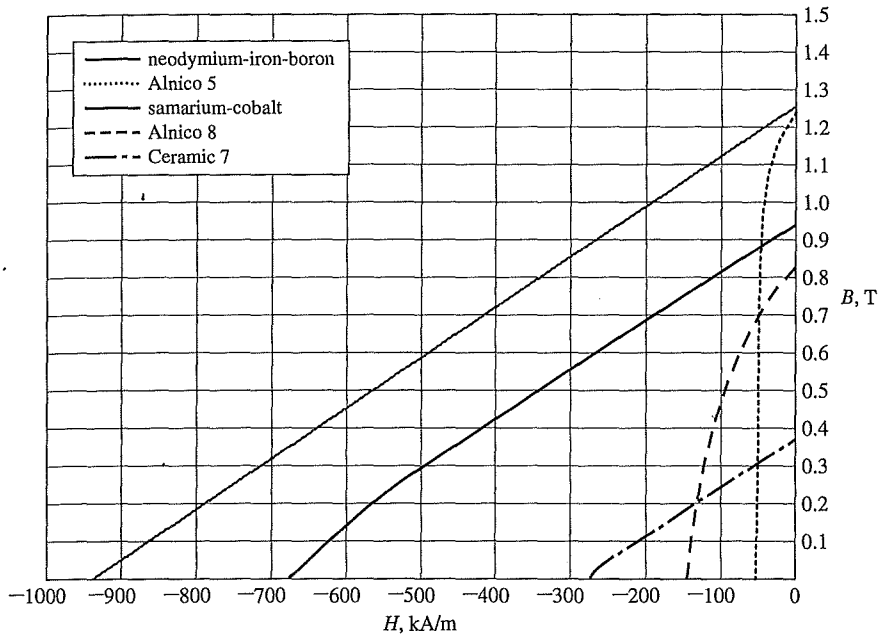

Figure 1.19 Magnetization curves for common permanent-magnet materials.

materials involved. In fact, in practical engineering devices, the situation is often more complex.[10] This section will expand upon these issues.

Figure 1.19 shows the magnetization characteristics for a few common permanent-magnet materials. These curves are simply the second-quadrant characteristics of the hysteresis loops for each material obtained when the material is driven heavily into saturation. Alnico 5 is a widely-used alloy of iron, nickel, aluminum, and cobalt originally discovered in 1931. It has a relatively large residual flux density. Alnico 8 has a lower residual flux density and a higher coercivity than Alnico 5. It is hence less subject to demagnetization than Alnico 5. Disadvantages of the Alnico materials are their relatively low coercivity and their mechanical brittleness.

Ceramic permanent-magnet materials (also known as *ferrite magnets*) are made from iron-oxide and barium- or strontium-carbonate powders and have lower residual flux densities than Alnico materials but significantly higher coercivities. As a result, they are much less prone to demagnetization. One such material, Ceramic 7, is shown in Fig. 1.19, where its magnetization characteristic is almost a straight line. Ceramic magnets have good mechanical characteristics and are inexpensive to manufacture.

[10]For a further discussion of permanent magnets and their application, see P. Campbell, *Permanent Magnet Materials and Their Application*, Cambridge University Press, 1994; R.J. Parker, *Advances in Permanent Magnetism*, John Wiley & Sons, 1990; R.C. O'Handley, *Modern Magnetic Materials: Principles and Applications*, John Wiley & Sons, 2000; and E.P. Ferlani, *Permanent Magnet and Electromechanical Devices*, Academic Press, 2001.

Samarium-cobalt represents a significant advance in permanent-magnet technology which began in the 1960s with the discovery of rare-earth permanent-magnet materials. From Fig. 1.19 it can be seen to have a high residual flux density such as is found with the Alnico materials, while at the same time having a much higher coercivity and maximum energy product.

The newest of the rare-earth magnetic materials is the family of neodymium-iron-boron materials. They feature even larger residual flux density, coercivity, and maximum energy product than does samarium-cobalt. The development of neodymium-iron-boron magnets has had a tremendous impact in the area of rotating machines and as a result permanent-magnet motors with increasingly large ratings are being developed by manufacturers around the world.

Note that in Fig. 1.19 the hysteretic nature of the magnetization characteristics of Alnico 5 and Alnico 8 is readily apparent while the magnetization characteristics of the remaining materials appear to be essentially straight lines. This straight-line characteristic is deceiving; in each case the material characteristic bends sharply downward just as does that of the Alnico materials. However, unlike the Alnico materials, this bend, commonly referred to as the *knee* of the magnetization curve, occurs in the third quadrant and hence does not appear in Fig. 1.19.

Consider the magnetic circuit of Fig. 1.20. This includes a section of hard magnetic material in a core of highly permeable soft magnetic material as well as an N-turn excitation winding. With reference to Fig. 1.21, we assume that the hard magnetic material is initially unmagnetized (corresponding to point (a) of the figure) and consider what happens as current is applied to the excitation winding. Because the core is assumed to be of infinite permeability, the horizontal axis of Fig. 1.21 can be considered to be both a measure of the applied current $i = Hl_m/N$ as well as a measure of H in the magnetic material.

As the current i is increased to its maximum value, the B-H trajectory rises from point (a) in Fig. 1.21 toward its maximum value at point (b). To fully magnetize the material, we assume that the current has been increased to a value i_{max} sufficiently large

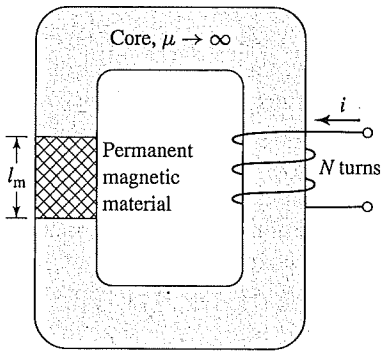

Figure 1.20 Magnetic circuit including both a permanent magnet and an excitation winding.

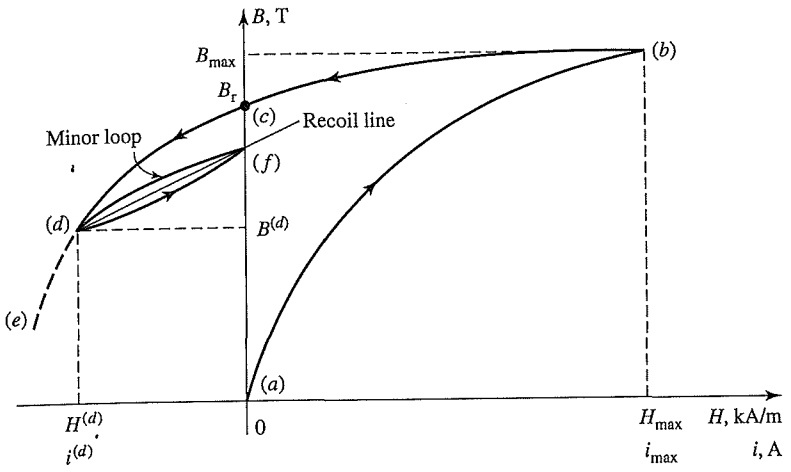

Figure 1.21 Portion of a *B-H* characteristic showing a minor loop and a recoil line.

that the material has been driven well into saturation at point (b). When the current is then decreased to zero, the *B-H* characteristic will begin to form a hysteresis loop, arriving at point (c) at zero current. At point (c), notice that H in the material is zero but B is at its remanent value B_r.

As the current then goes negative, the *B-H* characteristic continues to trace out a hysteresis loop. In Fig. 1.21, this is seen as the trajectory between points (c) and (d). If the current is then maintained at the value $i^{(d)}$, the operating point of the magnet will be that of point (d). Note that, as in Example 1.9, this same operating point would be reached if the material were to start at point (c) and, with the excitation held at zero, an air gap of length $g = l_m(A_g/A_m)(-\mu_0 H^{(d)}/B^{(d)})$ were then inserted in the core.

Should the current then be made more negative, the trajectory would continue tracing out the hysteresis loop toward point (e). However, if instead the current is returned to zero, the trajectory does not in general retrace the hysteresis loop toward point (c). Rather it begins to trace out a *minor hysteresis loop*, reaching point (f) when the current reaches zero. If the current is then varied between zero and $i^{(d)}$, the *B-H* characteristic will trace out the minor loop as shown.

As can be seen from Fig. 1.21, the *B-H* trajectory between points (d) and (f) can be represented by a straight line, known as the *recoil line*. The slope of this line is called the *recoil permeability* μ_R. We see that once this material has been demagnetized to point (d), the effective residual magnetization of the magnetic material is that of point (f) which is less than the residual magnetization B_r which would be expected based on the hysteresis loop. Note that should the demagnetization be decreased past point (d), for example, to point (e) of Fig. 1.21, a new minor loop will be created, with a new recoil line and recoil permeability.

The demagnetization effects of negative excitation which have just been discussed are equivalent to those of an air gap in the magnetic circuit. For example, clearly the

magnetic circuit of Fig. 1.20 could be used as a system to magnetize hard magnetic materials. The process would simply require that a large excitation be applied to the winding and then reduced to zero, leaving the material at a residual magnetization B_r (point (c) in Fig. 1.21).

Following this magnetization process, if the material were removed from the core, this would be equivalent to opening a large air gap in the magnetic circuit, demagnetizing the material in a fashion similar to that seen in Example 1.9. At this point, the magnet has been effectively weakened, since if it were again inserted in the magnetic core, it would follow a recoil line and return to a residual magnetization somewhat less than B_r. As a result, hard magnetic materials, such as the Alnico materials of Fig. 1.19, often do not operate stably in situations with varying mmf and geometry, and there is often the risk that improper operation can significantly demagnetize them.

At the expense of a reduction in value of the residual magnetization, hard magnetic materials such as Alnico 5 can be stabilized to operate over a specified region. This procedure, based on the recoil trajectory shown in Fig. 1.21, can best be illustrated by an example.

EXAMPLE 1.11

Figure 1.22 shows a magnetic circuit containing hard magnetic material, a core and plunger of high (assumed infinite) permeability, and a 100-turn winding which will be used to magnetize the hard magnetic material. The winding will be removed after the system is magnetized. The plunger moves in the x direction as indicated, with the result that the air-gap area varies over the range $2\ \text{cm}^2 \le A_g \le 4\ \text{cm}^2$. Assuming that the hard magnetic material is Alnico 5 and that the system is initially magnetized with $A_g = 2$ cm, (a) find the magnet length l_m such that the system will operate on a recoil line which intersects the maximum B-H product point on the magnetization curve for Alnico 5, (b) devise a procedure for magnetizing the magnet, and (c) calculate the flux density B_g in the air gap as the plunger moves back and forth and the air gap varies between these two limits.

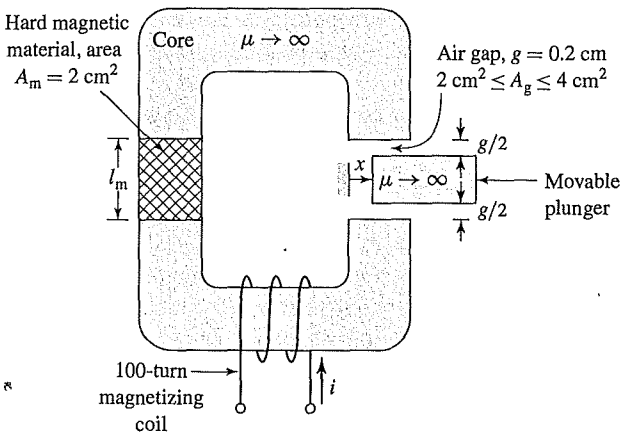

Figure 1.22 Magnetic circuit for Example 1.11.

Solution

a. Figure 1.23a shows the magnetization curve for Alnico 5 and two load lines corresponding to the two extremes of the air gap, $A_g = 2\ \text{cm}^2$ and $A_g = 4\ \text{cm}^2$. We see that the system will operate on the desired recoil line if the load line for $A_g = 2\ \text{cm}^2$ intersects the B-H characteristic at the maximum energy product point (labeled point (a) in Fig. 1.23a), $B_m^{(a)} = 1.0$ T and $H_m^{(a)} = -40$ kA/m.

From Eqs. 1.56 and 1.57, we see that the slope of the required load line is given by

$$\frac{B_m^{(a)}}{-H_m^{(a)}} = \frac{B_g}{H_g}\frac{A_g}{A_m}\frac{l_m}{g}$$

and thus

$$l_m = g\left(\frac{A_m}{A_g}\right)\left(\frac{B_m^{(a)}}{-\mu_0 H_m^{(a)}}\right)$$

$$= 0.2\ \text{cm}\left(\frac{2}{2}\right)\left(\frac{1.0}{4\pi \times 10^{-7} \times 4 \times 10^4}\right) = 3.98\ \text{cm}$$

b. Figure 1.23b shows a series of load lines for the system with $A_g = 2\ \text{cm}^2$ and with current i applied to the excitation winding. The general equation for these load lines can be readily derived since from Eq. 1.5

$$Ni = H_m l_m + H_g g$$

and from Eqs. 1.3 and 1.7

$$B_m A_m = B_g A_g = \mu_0 H_g A_g$$

Thus

$$B_m = -\mu_0\left(\frac{A_g}{A_m}\right)\left(\frac{l_m}{g}\right)H_m + \frac{\mu_0 N}{g}\left(\frac{A_g}{A_m}\right)i$$

$$= \mu_0\left[-\left(\frac{2}{2}\right)\left(\frac{3.98}{0.2}\right)H_m + \frac{100}{2 \times 10^{-3}}\left(\frac{2}{2}\right)i\right]$$

$$= -2.50 \times 10^{-5} H_m + 6.28 \times 10^{-2} i$$

From this equation and Fig. 1.23b, we see that to drive the magnetic material into saturation to the point (H_{max}, B_{max}), the current in the magnetizing winding must be increased to the value i_{max} where

$$i_{max} = \frac{B_{max} + 2.50 \times 10^{-5} H_{max}}{6.28 \times 10^{-2}} \quad \text{A}$$

In this case, we do not have a complete hysteresis loop for Alnico 5, and hence we will have to estimate B_{max} and H_{max}. Linearly extrapolating the B-H curve at $H = 0$ back to 4 times the coercivity, that is, $H_{max} = 4 \times 50 = 200$ kA/m, yields $B_{max} = 2.1$ T. This value is undoubtedly extreme and will overestimate the required current somewhat. However, using $B_{max} = 2.1$ T and $H_{max} = 200$ kA/m yields $i_{max} = 113$ A.

Thus with the air-gap area set to 2 cm^2, increasing the current to 113 A and then reducing it to zero will achieve the desired magnetization.

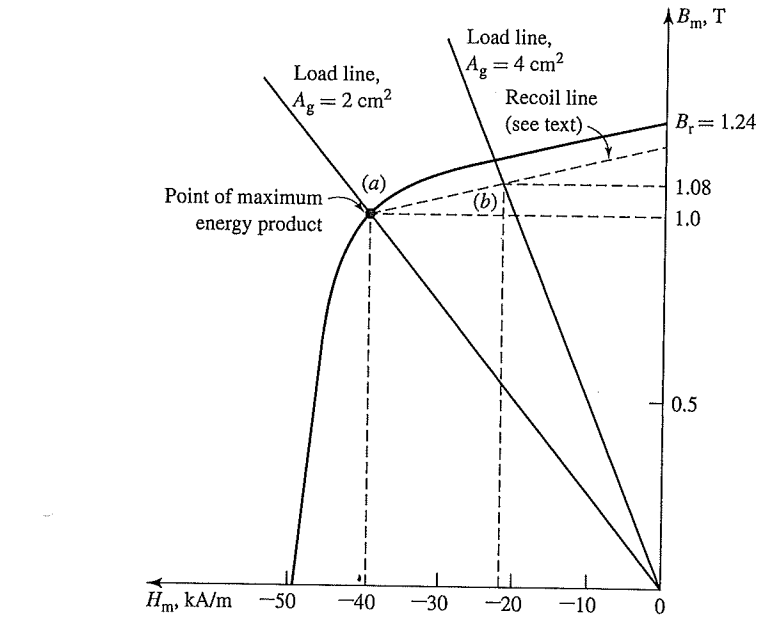

(a)

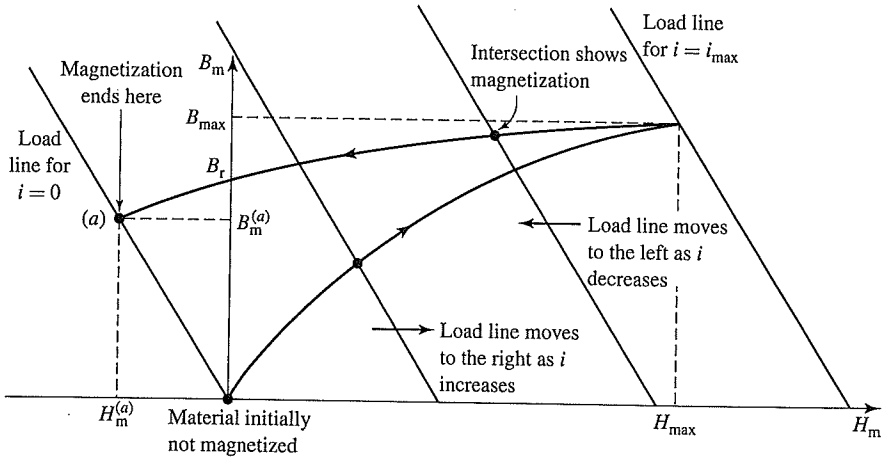

(b)

Figure 1.23 (a) Magnetization curve for Alnico 5 for Example 1.11; (b) series of load lines for $A_g = 2$ cm^2 and varying values of i showing the magnetization procedure for Example 1.11.

c. Because we do not have specific information about the slope of the recoil line, we shall assume that its slope is the same as that of the B-H characteristic at the point $H = 0$, $B = B_r$. From Fig. 1.23a, with the recoil line drawn with this slope, we see that as the air-gap area varies between 2 and 4 cm^2, the magnet flux density B_m varies between 1.00

and 1.08 T. Since the air-gap flux density equals A_m/A_g times this value, the air-gap flux density will equal (2/2)1.00 = 1.0 T when $A_g = 2.0\text{cm}^2$ and (2/4)1.08 = 0.54 T when $A_g = 4.0\ \text{cm}^2$. Note from Fig. 1.23a that, when operated with these air-gap variations, the magnet appears to have an effective residual flux density of 1.17 T instead of the initial value of 1.24 T. As long as the air-gap variations limited to the range considered here, the system will continue to operate on the line labeled "Recoil line" in Fig. 1.23a and the magnet can be said to be *stabilized.*

As has been discussed, hard magnetic materials such as Alnico 5 can be subject to demagnetization, should their operating point be varied excessively. As shown in Example 1.11, these materials can be stabilized with some loss in effective residual magnetization. However, this procedure does not guarantee absolute stability of operation. For example, if the material in Example 1.11 were subjected to an air-gap area smaller than 2 cm^2 or to excessive demagnetizing current, the effect of the stabilization would be erased and the material would be found to operate on a new recoil line with further reduced magnetization.

However, many materials, such as samarium-cobalt, Ceramic 7, and neodymium-iron-boron (see Fig. 1.19), which have large values of coercivity, tend to have very low values of recoil permeability, and the recoil line is essentially tangent to the *B-H* characteristic for a large portion of the useful operating region. For example, this can be seen in Fig. 1.19, which shows the dc magnetization curve for neodymium-iron-boron, from which we see that this material has a residual magnetization of 1.25 T and a coercivity of −940 kA/m. The portion of the curve between these points is a straight line with a slope equal to $1.06\mu_0$, which is the same as the slope of its recoil line. As long as these materials are operated on this low-incremental-permeability portion of their *B-H* characteristic, they do not require stabilization, provided they are not excessively demagnetized.

For these materials, it is often convenient to assume that their dc magnetization curve is linear over their useful operating range with a slope equal to the recoil permeability μ_R. Under this assumption, the dc magnetization curve for these materials can be written in the form

$$B = \mu_R(H - H_c') = B_r + \mu_R H \tag{1.60}$$

Here, H_c' is the *apparent coercivity* associated with this linear representation. As can be seen from Fig. 1.19, the apparent coercivity is typically somewhat larger in magnitude (i.e. a larger negative value) than the material coercivity H_c because the dc magnetization characteristic tends to bend downward for low values of flux density.

A significant (and somewhat unfortunate) characteristic of permanent-magnet materials is that their properties are temperature dependent. For example, the residual magnetization and coercivity of neodymium-iron-boron and samarium-cobalt magnets decrease as the temperature increases, although samarium-cobalt is much less temperature sensitive than neodymium-iron-boron.

Figure 1.24 shows magnetization curves for a high-temperature grade of neodymium-boron-iron at various temperatures. We see that the residual magnetism

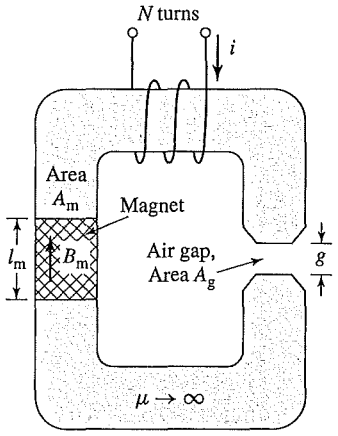

Figure 1.26 Magnetic circuit with a permanent magnet, an air gap and an excitation winding.

This can be seen in the curves for 180 C and 210 C in Fig. 1.24. In the case of the 180 C characteristic, the winding current can be varied without demagnetizing the magnet as long as the magnet flux density does not drop below the point where the magnetization characteristic becomes non linear. Operation below this point is analogous to the operation of Alnico 5 as discussed with reference to the minor loop and recoil line of Fig. 1.21. Thus, if sufficient winding current is applied to drive the magnet below this point and the current is then reduced, a minor loop will be created and the magnet will be somewhat demagnetized. If the magnet temperature is reduced, the magnet will be found to be partially demagnetized. In the case of the 210 C characteristic, we see that the zero-excitation operating point falls in the non-linear portion of the magnetization current. As a result, any winding current which causes an increase in magnet flux density will demagnetize the magnet.

EXAMPLE 1.12

A magnetic circuit similar to that of Fig. 1.26 has a 200-turn winding ($N = 200$) and includes a neodymium-boron-iron magnet of length $l_m = 3$ cm and cross-sectional area $A_m = 2.5$ cm^2. The airgap has an effective area of $A_g = 0.259$ cm^2 and an effective length of $g = 0.9$ cm.

a. Derive an expression for the load-line of this magnetic circuit as a function of winding current i and show that it coincides with the zero-excitation load line of Fig. 1.24 when the winding current is equal to zero.

b. The magnetic circuit is excited by a sinusoidal winding current of peak amplitude I_{peak}. In order to avoid the possibility of demagnetizing the magnet, it is desirable to limit I_{peak} to a value such that the magnet flux density B_m remains positive. Calculate the maximum amplitude of I_{peak} for magnet operating temperatures of 20 C and 120 C.

Solution

a. This magnetic circuit is essentially identical to that of Example 1.11 and Fig. 1.22. Hence the equation for the load line is identical to that derived in that example. Specifically,

$$B_m = -\mu_0 \left(\frac{A_g}{A_m}\right)\left(\frac{l_m}{g}\right) H_m + \frac{\mu_0 N}{g}\left(\frac{A_g}{A_m}\right) i$$

$$= \mu_0 \left[-\left(\frac{0.259}{2.5}\right)\left(\frac{3}{0.9}\right) H_m + \frac{200}{9 \times 10^{-3}}\left(\frac{0.259}{2.5}\right) i\right]$$

$$= -4.34 \times 10^{-7} H_m + 2.89 \times 10^{-3} i$$

With $i = 0$, when $H_m = -600$ kA/m, this equation gives $B_m = 0.26$ T which closely coincides with the zero-excitation load line of Fig 1.24.

b. From Eq.1.60, over the linear operating region the relationship between B_M and H_m in the magnet is given by

$$B_m = B_r + \mu_R H_m$$

Combining this expression with the equation for the load-line of part (a) gives

$$B_m = \frac{\mu_R N i + l_m B_r}{l_m + g\left(\frac{\mu_R}{\mu_0}\right)\left(\frac{A_m}{A_g}\right)} = 2.17 \times 10^{-3} i + 0.249 B_r$$

For a sinusoidal current of peak amplitude I_{peak}, B_m will remain positive as long as

$$I_{peak} = \frac{l_m B_r}{\mu_R N} = 114.8 B_r$$

For a temperature of 80 C, from Table 1.1 $B_r = 1.15$ T and thus the maximum value of I_{peak} is 132 A. Similarly, for a temperature of 120 C, $B_r = 1.03$ and the maximum value of I_{peak} is 118 A.

1.7 SUMMARY

Electromechanical devices which employ magnetic fields often use ferromagnetic materials for guiding and concentrating these fields. Because the magnetic permeability of ferromagnetic materials can be large (up to tens of thousands times that of the surrounding space), most of the magnetic flux is confined to fairly well-defined paths determined by the geometry of the magnetic material. In addition, often the frequencies of interest are low enough to permit the magnetic fields to be considered quasi-static, and hence they can be determined simply from a knowledge of the net mmf acting on the magnetic structure.

As a result, the solution for the magnetic fields in these structures can be obtained in a straightforward fashion by using the techniques of magnetic-circuit analysis. These techniques can be used to reduce a complex three-dimensional magnetic field solution to what is essentially a one-dimensional problem. As in all engineering solutions, a certain amount of experience and judgment is required, but the technique gives useful results in many situations of practical engineering interest.

Ferromagnetic materials are available with a wide variety of characteristics. In general, their behavior is nonlinear, and their B-H characteristics are often represented in the form of a family of hysteresis (B-H) loops. Losses, both hysteretic and eddy-current, are functions of the flux level and frequency of operation as well as the material composition and the manufacturing process used. A basic understanding of the nature of these phenomena is extremely useful in the application of these materials in practical devices. Typically, important properties are available in the form of curves supplied by the material manufacturers.

Certain magnetic materials, commonly known as hard or permanent-magnet materials, are characterized by large values of residual magnetization and coercivity. These materials produce significant magnetic flux even in magnetic circuits with air gaps. With proper design they can be made to operate stably in situations which subject them to a wide range of mmfs and temperature variations. Permanent magnets find application in many small devices, including loudspeakers, ac and dc motors, microphones, and analog electric meters.

1.8 CHAPTER 1 VARIABLES

μ	Magnetic permeability [H/m]
μ_0	Permeability of free space $= 4\pi \times 10^{-7}$ [H/m]
μ_r	Relative permeability
μ_R	Recoil permeability [H/m]
$\phi, \varphi, \phi_{max}$	Magnetic flux [Wb]
ω	Angular frequency [rad/sec]
ρ	Mass density [kg/m^3]
A	Cross-sectional area [m^2]
$\mathbf{B}, B$	Magnetic flux density [T]
B_r	Residual/remanent magnetization [T]
e	Electromotive force [V]
e, E	Voltage [V]
$\mathbf{E}$	Electric field intensity [V/m]
f	Frequency [Hz]
$\mathcal{F}$	Magnetomotive force [A]
g	Gap length [m]
$\mathbf{H}, H, H_{rms}$	Magnetic field intensity [A/m]
H_c	Coercivity [A/m]
i, I	Current [A]
$i_\varphi, I_{\phi,rms}$	Exciting current [A]
$\mathbf{J}$	Current density [A/m^2]
l	Linear dimension [m]
L	Inductance [H]
N	Number of turns
P	Power [W]
P_{core}	Core loss [W]
P_a	Exciting rms voltamperes per unit mass [W/kg]

P_c	Core loss density [W/kg]
$\mathcal{P}$	Permeance [H]
R	Resistance [Ω]
$\mathcal{R}$	Reluctance [H^{-1}]
S	Exciting rms voltamperes [VA]
S_a	Exciting rms voltamperes per mass [VA/kg]
t	Time [sec]
T	Period [sec]
T	Temperature [C]
V	Voltage [V]
Vol	Volume [m^3]
W	Energy [J]

Subscripts:

c	Core
g	Gap
m, mag	Magnet
max	Maximum
rms	Root mean square
tot	Total

1.9 PROBLEMS

1.1 A magnetic circuit with a single air gap is shown in Fig. 1.27. The core dimensions are

Cross-sectional Area $A_c = 3.5$ cm^2
Mean core length $l_c = 25$ cm
Gap length $g = 2.4$ mm
$N = 95$ turns

Assume that the core is of infinite permeability ($\mu \to \infty$) and neglect the effects of fringing fields at the air gap and leakage flux. (a) Calculate the reluctance of the core $\mathcal{R}_c$ and that of the gap $\mathcal{R}_g$. For a current of $i = 1.4$ A, calculate (b) the total flux ϕ, (c) the flux linkages λ of the coil, and (d) the coil inductance L.

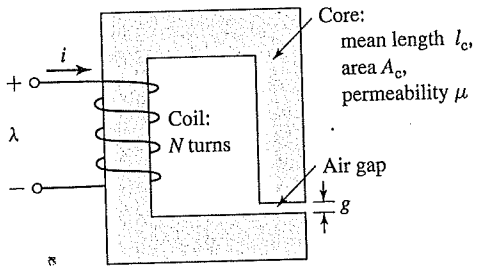

Figure 1.27 Magnetic circuit for Problem 1.1.